Fall 9-11-2017

Development of Markers for Embryonic Reproductive Competence in Assisted Reproduction

Xin Tao
xin.tao@student.shu.edu

DEVELOPMENT OF MARKERS FOR EMBRYONIC REPRODUCTIVE COMPETENCE IN ASSISTED REPRODUCTION

BY

XIN TAO

Submitted in partial fulfillment of the requirements for the
degree of Doctor of Philosophy in Molecular Bioscience from the
Department of Biological Sciences of Seton Hall University

September 2017

APPROVED BY

Co-MENTOR
Dr. Tinchun Chu

Co-MENTOR
Dr. Nathan R. Treff

COMMITTEE MEMBER
Dr. Jane L. Ko

COMMITTEE MEMBER
Dr. Angela V. Klaus

COMMITTEE MEMBER
Dr. Daniel B. Nichols

COMMITTEE MEMBER
Dr. Eric J. Forman

DIRECTOR OF GRADUATE STUDIES
Dr. Angela V. Klaus

CHAIRPERSON, DEPARTMENT OF BIOLOGICAL SCIENCES
Dr. Heping Zhou

ACKNOWLEDGEMENTS

I would like to gratefully and sincerely thank my mentor, **Dr. Tinchun Chu** for her guidance and understanding during my graduate studies at Seton Hall University. Her patience, flexibility, genuine caring and concern, and faith in me during the dissertation process enabled me to attend to life while also earning my Ph.D. She's always been motivating, encouraging and enlightening. For this, I cannot thank her enough. I am forever grateful. Thank You Dr. Chu!

I'd also like to give a heartfelt, special thanks to **Dr. Nathan R. Treff** for being my mentor. Dr. Treff has blessed me with believing in me to succeed both academically as well as in my professional career, and for that I will be eternally grateful. I cannot thank him enough for his support and aid in the completion of this project. It's been such a pleasure to work with him.

I would also like to express my thankfulness to my committee members, **Dr. Jane L. Ko, Dr. Angela Klaus, Dr. Daniel B. Nichols** and **Dr. Eric J. Forman** for all their valuable time, comments and advice during this study and while reviewing my dissertation.

I would like to take this opportunity to thank **Dr. Richard T. Scott Jr.** for all his support, encouragement and helpful advice. I would also like to thank all the physicians, nurses and embryologists at RMANJ, especially **Dr. Jason M. Franasiak**, for recruiting patients and collecting samples for my dissertation.

I would like to thank the bioinformatics team at the Foundation for Embryonic Competence, **Dr. Yiping Zhan, Dr. Jessica Landis** and **Dr. Li** Sun for the data analysis support. I would also express my thankfulness to **Dr. Deanne Taylor**, the previous director of bioinformatics department, for the data analysis support.

My sincere thanks also goes to the **Chaim Jalas**, the COO of the Foundation for Embryonic Competence for his support.

I am very grateful to my team members, **Leslie Duffy, Jessica Rajchel, Jenna Bedard, Richard T Scott III, Diego Marin, Heather Garnsey, Anna Czyrsznic, Margaret Lebiedzinski,** and **Oksana Bendarsky** at the Foundation for Embryonic Competence for encouragement, technical assistance and moral support.

Robert Newby, Jr. and **Jose L. Perez**, my fellow research peers at Seton Hall University, thank you for your endless support.

Finally, I am forever indebted to my family, especially my father **Xiyu Tao**, my mother **Yingfang Zhou**, and my husband **Qingfeng Li**, for their love, understanding, endless patience, and encouragement when it was most required.

TABLE OF CONTENTS

LIST OF FIGURES

LIST OF TABLES

Abstract

In humans, early embryo development is a complex process that consists of sequential events: oocyte maturation, fertilization, embryonic growth and implantation. Disruption of these highly regulated processes results in reproductive failure and infertility. This study characterizes and describes embryonic aneuploidy, mitochondrial content level and endometrial microbial environment related to reproductive competence, in particular instances in which failure results.

To examine the molecular underpinnings of mammalian gamete and early embryo chromosome segregation, we established a comprehensive chromosomal screening (CCS) method for mice poly bodies, oocytes and embryos by the application of whole genome amplification (WGA) and next generation sequencing (NGS). First, we validated this approach using single mouse embryonic fibroblasts engineered to have stable trisomy 16. We further validated this method by identifying reciprocal chromosome segregation errors in the products of meiosis I (gamete and polar body) in oocytes from reproductively aged mice. Finally, we applied this technology to investigate the incidence of aneuploidy in IVM- and IVF- derived blastocysts from both young and reproductively aged mice.

It was reported that mtDNA was significantly increased in aneuploid human embryos compared to euploid embryos and also associated with maternal age. In this study, we established the mouse model of mitochondrial DNA (mtDNA) quantitation in reproductive samples based on WGA and NGS. The method was validated on a tumor-derived mouse cell line, and then applied to mouse reproductive samples. Cells in blastocysts from younger mice contained significantly lower amounts of mtDNA compared to aged mice ($P<0.001$). Cells in blastocysts produced via IVO had higher mtDNA content than IVM-derived blastocysts ($P=0.0052$). Cells in aneuploid blastocysts were found to have significantly higher (1.74-fold) levels of mtDNA compared to

euploid blastocysts (P=0.0045). WGA and NGS provided a reliable method to assess mtDNA content in mouse gametes and embryos. We also established a quantitative method to detect mtDNA copy number in human embryos. The maternal age of the embryos displayed a significant correlation with mtDNA content (p=0.007). This well controlled study demonstrated that mtDNA quantitation provided no additional selection advantage between euploid sibling embryos in a double embryo transfer model.

There is growing interest in the microbiome of the reproductive tract. The vaginal and placental microbiome have been partially characterized and shown to be related to obstetric outcomes. In this study, we assessed the quality of Ion PGM- and Illumina MiSeq-generated data for 16S rRNA metagenomics, established the sensitivity of Illumnia 16S V4 metagenomics, then studied the endometrial microbial environment by analyzing the embryo transfer (ET) tip after embryo transfer. There were a total of 248 genera detected amongst all specimens. Lactobacillus genera were detected in all of the samples. When analyzing fraction of lactobacillus reads, there were no differences (p=0.464) The Shannon Diversity Index did not differ between the two groups (p=0.164). The data in this study showed the microbiome at the time of ET may differ by pregnancy outcome but highlighted the challenge of low bacterial load and read counts when analyzing ET catheter tips alone.

Keywords:

IVF, aneuploidy, aging, embryo, oocytes, comprehensive chromosome screening, mitochondrial DNA, NGS, microbiome, 16S rRNA.

Introduction

Infertility is the inability to get pregnant after at least 12 consecutive months of appropriately times, unprotected intercourse. There are over 1.5 million women ages 15-44 that are infertile in the USA, which represented 6.0% of the population in 2006-2010[1]. Age alone has an effect on fertility by reducing the production of oocyes[2,3] and decreasing the quality of oocytes[4]. Oocyte quality is dictated by acquisition of both meiotic and cytoplasmic competence[5]. The implantation failure of euploid embryos also relates to the uterine endometrial microbial environment of the patient[6]. In this study, we investigate aneuploidy associated with meiotic competence, mitochondrial level related to cytoplasmic competence and endometrial microbiome on the day of embryo transfer.

Mouse aneuploidy model and Reproductive Competence

In humans, early embryo development is a complex process that consists of sequential events: oocyte maturation, fertilization, embryonic growth and implantation. Disruption of these highly regulated processes results in reproductive failure and infertility. Advances in clinical and laboratory practice have resulted in steady improvements in in vitro fertilization (IVF) outcomes since the birth of the first IVF baby in 1978. However, this technique remains inefficient.

Much of assisted reproductive technology success depends on the oocyte quality achieved during the maturation process[7] as well as the inflammatory and immune milieu at the time of embryo implantation. Oocyte quality involves primarily acquisition of both meiotic and cytoplasmic competence[8]. Meiotic competence refers to the ability of the oocyte to reverse meiotic arrest at prophase I and drive the progress of meiosis to produce a haploid gamete[9]. Errors in this process leads to aneuploidy, which is the leading cause of failed implantation, miscarriage, and can result

in congenital birth defects[10]. Indeed, chromosomal abnormalities are likely the most prevalent cause of failed reproductive competence in human embryos[11]. Cytoplasmic competence refers to the ability of the oocyte to accumulate critical stores of maternally derived proteins, mRNAs, and organelles, most prominent of which are the mitochondria, during oogenesis. This process is essential for preparing the egg for activation and preimplantation development[12].

Use of comprehensive aneuploidy screening (CCS) in clinical Assisted Reproductive Technology (ART) has shown that advanced reproductive age is associated with increased aneuploidy, largely due to chromosome segregation errors in the oocyte during meiosis[13]. The age-related decline in fertility is accompanied by significant increases in the rate of aneuploidy, which contributes to adverse reproductive outcomes including miscarriages, infertility, and birth defects[14]. It is critical to understanding the mechanism of aneuploidy associated with age because of the increased maternal age in the United States[15].

Model organisms allow for better understanding the aneuploidy mechanisms without the added risk of harming an actual human embryo. Polar body biopsy may impair on human embryonic implantation potential and it is not feasible to study human oocytes due to direct testing a human oocyte would destroy its potential for IVF. In an animal model, all the reproductive samples can be studied to discover the aneuploidy mechanisms.

The age-related increase in aneuploidy has been observed in both human and mouse. The aneuploidy rate increased from 3% to 60% in 1-month-old versus 15-month-old mice[16], mirroring the incidence of common age-associated trisomies in human oocytes[17]. Therefore, mice have the potential to be a useful model system to study origins/etiology/mechanisms of human aneuploidy. Most studies for evaluating aneuploidy in mouse gametes and early embryos are based on chromosome spreads and FISH[18]. These methods are technically challenging, and

not all the chromosomes can be reliably and efficiently detected in single cells, which put limitations on the mouse studies. An affordable method for comprehensive and chromosome-specific evaluation of aneuploidy in individual mouse cells is needed.

Methods of preimplantation comprehensive chromosome screening of human embryos has been well established and widely used in clinical ART to improve the outcome. The successful rate of IVF outcome has improved with the application of CCS in ART. The transfer of euploid embryos selected by CCS has improved the implantation rate from 47.9% to 66.4% and delivery rate from 67.5% to 84.7% in a well-designed randomized clinic trial[19]. Those methods incorporate an amplification of a targeted region or whole genome first. Quantitative real-time PCR(qPCR) is used to access aneuploidy for targeted amplification[20]. However, the targeted amplification requires the design and validation of species-specific primers. Array comparative genomic hybridization (array CGH), single nucleotide polymorphism (SNP) arrays, or next generation sequencing (NGS) can be used to access aneuploidy for whole genome amplification (WGA)[21]. Of note, array CGH and SNP array also require species-specific design due to the special probes required. One advantage of using WGA and NGS is the ability to amplify and analyze DNA from any species, and the copy number of each chromosome can be calculated based on normal male references. This study is establishing a comprehensive chromosomal screening method for mice poly bodies, oocytes and embryos by application of WGA and NGS. This technology can be applied to discover the mechanism of aneuploidy associated with age in mammals.

This is the first time WGA and NGS have been applied to comprehensively screen aneuploidies in individual mouse reproductive oocytes, polar bodies and embryos. This method overcomes the technical challenges associated with fluorescence in situ hybridization (FISH) which led to poor

accuracy and reproducibility, as well as the ability to assess only a limited number of chromosomes with FISH technology. This strategy provides the fields of reproductive science and medicine with a new research tool to improve the basic understanding of mechanisms contributing to maternal age-associated aneuploidy in mammals. The mouse model can be used to assess meiotic and mitotic segregation errors, distinguish aneuploidy due to premature separation of sister chromatids and classical non-disjunction, and evaluate the aneuploidy rate affected by age, drugs, environmental factors, and disease conditions.

Mitochondria in Reproductive Competence

The success of *in vitro* fertilization (IVF) has increased greatly with the application of comprehensive chromosome screening (CCS) in Assisted Reproductive Technology (ART). The transfer of euploid embryos selected by CCS improved the implantation rate from 47.9% to 66.4% and delivery rate from 67.5% to 84.7% in a well-designed randomized clinical trial[22]. However, not every transferred euploid embryo results in implantation and delivery because embryo competence is also related to cytoplasmic content[23].

Mitochondria are well-defined cytoplasmic organelles that produce the energy currency (adenosine triphosphate; ATP) of the cell through respiration and regulate cellular metabolism[24]. Mitochondria are also an important source of reactive oxygen species (ROS) from complexes I and III of the electron transport chain[25], which cause oxidative stress in the mitochondria and may contribute to the decline in mitochondrial function associated with the aging process[26]. In addition to supplying cellular energy, mitochondria are involved in other tasks, such as signaling, cellular differentiation, and cell death, as well as maintaining control of the cell cycle and cell growth. Unlike other cell organelles, mitochondria contain their own genome. Each mitochondrion is estimated to contain 2-10 mtDNA copies[27]. Eighty percent of mitochondrial

DNA codes for mitochondrial RNA, and therefore most mitochondrial DNA disorders lead to functional problems. The mtDNA copy number in early embryonic development has become the subject of a number of clinical and basic studies. It was reported that mtDNA was significantly increased in aneuploid human embryos compared to euploid embryos[28] and associated with maternal age[29]. The less mtDNA content in embryos was an indicator for better embryonic implantation potential[30,31]. However, the underlying mechanism remains largely unknown.

Research on early embryo development using model organisms obviates the need for using human eggs and preimplantation embryos, which would destroy their potential use for IVF and may not be feasible due to ethical and legal restrictions. Animal models also have the benefit of reduced genetic background variability. Mouse early embryo developmental stages are similar to those of the human embryo, and it is feasible to manipulate mouse embryos. Therefore, mice have the potential to be a useful model system to study the mtDNA levels as a biomarker in pre-implantation embryo development.

Previously, a method using whole genome amplification (WGA) and next generation sequencing (NGS) was developed for CCS of mouse reproductive samples[32]. We observed that increased aneuploidy was associated with advanced reproductive age, which was consistent with other studies[33,34,35]. The origin of aneuploidy is primarily attributed to errors during maternal meiosis in the oocyte[36]. The number of mitochondria increases sharply during oogenesis, and may play an important roles for aneuploidy.

In the previous study, we also observed that blastocysts derived via *in vitro* maturation (IVM) had a higher aneuploidy rate than the blastocysts produced via *in vivo* maturation (IVO)[32]. Oocyte maturation is the final phase of oogenesis which involves both nuclear and cytoplasmic maturation[37]. In IVO, this process involves a number of signaling pathways and depends on the

close interaction between the cumulus cells and the oocyte[38]. For IVM, while nuclear maturation is supported, cytoplasmic maturation is not assured[34]. The gradual accumulation of mitochondrial copy number and activity as oocyte development progresses is important for cytoplasmic maturation[39]. Understanding the association between blastocyst mtDNA level and the oocyte maturation methods will provide insight into cytoplasmic maturation under different maturation conditions.

In this study, we validated the WGA and NGS based mtDNA assessment on a tumor-derived mouse cell line with ethidium bromide (EtBr) treatment. EtBr impairs mtDNA replication, and mtDNA levels decrease upon exposure to EtBr[40]. After validating our method, relative mtDNA copy number in individual mouse reproductive samples including polar bodies, oocytes, and embryos were assessed, providing insight into mtDNA levels in the preimplantation embryo and their relationship with chromosomal ploidy status, maternal age, and oocyte maturation methods. A recent study demonstrated that relative mtDNA content was affected by embryo gender and ploidy[41], therefore, we implemented the correction based on gender and ploidy when the relative mtDNA content was evaluated.

This study also developed a qPCR based method to access the relative copy number of mtDNA in trophectoderm biopsies from human embryos. A recent study showed an increased amount of mtDNA in euploid embryos was related to poor implantation potential and may be indicative of reduced metabolic fuel during oocyte maturation[42].This study is based on single embryo transfer and compares the implanted and unimplanted embryos from different individuals. The variation among patients may have an impact on the results. With the application of embryonic DNA finger printing in our study, the implanted embryo for multiple embryo transfer can be identified[43, 44]. Our study compares the mitochondrial content in the euploid and aneuploidy

sibling embryos and implanted and nonimplanted transferred euploid sibling embryos from the same individual. This design within the same individual patients eliminates the variation from individuals, embryo incubation conditions, and different operators for the IVF cycles.

Endometrial Microbiome and Reproductive Competence

The human body contains over 10 times more microbial cells than human cells, and the human microbiome can significantly affect human physiology[45]. Disrupting microbial ecosystems has been linked to diseases and many disease processes disrupt the microbial ecosystems which make up the human microbiome[46]. The taxonomic identification of microorganisms is critical to our understanding of the microbiome's role in reproductive physiology and pathophysiology. Indeed, in the wake of the Human Genome Project, a "second human genome project" was proposed that would investigate the normal microbiome at various sites in order to understand its synergistic interactions with the host[47,48].

The human microbiome affects the inflammatory and immune response throughout the body and it is likely this interaction is important in human reproductive tracts at the time of embryo implantation. A recent 16S RNA sequencing based study showed that the vaginal microbiome on the day of embryo transfer in assisted reproductive technology (ART) affects pregnancy outcome[49]. However, little is known about this interaction in uterus to date.

It was widely assumed that the uterine cavity in non-pregnant women was a sterile environment; however, recent studies have proved this to be incorrect[50]. The human uterine endometrium is governed by a delicate balance of microbes, cellular immune response, and cytokines which regulate the endometrial receptivity of an embryo. A receptive endometrial lining is a rate-limiting step in embryonic implantation and is essential for sustaining a viable clinical pregnancy.

Characterization of the endometrial microbial environment could be important in understanding endometrial proliferation, embryo implantation, and development of early pregnancies. In this study, we characterized the endometrial microbial environment by analyzing the embryo transfer tip after embryo transfer.

A major concern when describing the human microbiome is ensuring that the diversity of species in a particular environment is properly captured and characterized. Previous culture based microbial studies significantly underrepresent the diversity in a particular microbiome; in fact, less than 1% of bacteria reliably grow and form colonies even in appropriate culture conditions resulting in significant underreporting of biodiversity[51]. Because of this, more recent data in metagenomics rely upon 16S ribosomal RNA (rRNA) gene sequencing. The key to utilizing the 16S gene is that it contains both conserved regions and hypervariable regions (V1-V9). The conserved regions can be used to design universal primers while the hypervariable regions allow for specific taxonomic distinction[52].

16S rRNA hypervariable regions exhibit different degrees of sequence diversity, and not every hypervariable region is able to distinguish among all bacteria with equal specificity. Ion 16S metagenomics workflow uses two primer pools to amplify seven hypervariable regions (V2, V3, V4, V6, V7, V8, and V9) of bacterial 16S rRNA. Illumina 16S metagenomics workflow can target any hypervariable regions. The most widely used 16S hypervariable regions include V4[53,54] and V3-V4[55,56] of the 16S rRNA gene. In this study, we assessed the quality of Ion PGM- and MiSeq-generated data and determine their advantages and disadvantages for 16S rRNA metagenomics.

The current sequencing based human microbiome studies require DNA isolation and nanograms of input DNA for library preparation[57,58]. Therefore, a large amount of starting bacteria is needed. However, certain environmental samples and/or human body samples may contain very limited

amount of bacteria. Analyzing ultra-low amount of bacteria is technically challenging because of the DNA loss in the purification procedure and requirement of input DNA amount for NGS. Some clinically relevant minority populations, including potentially pathogenic bacteria, might be missed because of the depth bias. Culturomics had been used to overcome the depth bias in metagenomics approaches[59,60]. However, a more sensitive method is in need for the low bacterial mass samples. Presently, there are no studies showing minimum number of bacterial cells from the environmental samples are required for taxonomic classification. In this study, we developed a method to prepare 16S V4 NGS library followed by lysis directly for ultra-low amount of bacteria with great sensitivity for the first time.

This technique was then utilized to analyze the embryo transfer catheter tip, which contains the ultra-low amount of bacteria after embryo transfer in an IVF cycle. The microbial profiling from the transfer catheter tip represents the microbial structure of human uterine endometrium at the time of embryo transfer. The human uterine endometrium is governed by a delicate balance of microbes, cellular immune response, and cytokines which regulate the endometrial receptivity of an embryo. A receptive endometrial lining is a rate-limiting step in embryonic implantation and is essential for sustaining a viable clinical pregnancy. Characterization of the endometrial microbial environment could be important in understanding endometrial proliferation, embryo implantation, and development of early pregnancies.

Materials and Methods

Aim 1: Establishment of CCS for mouse model

Phase I: validation of WGA and NGS in individual mouse cells.

Cell lines

Cell lines include previously characterized mouse embryonic fibroblasts with trisomy 16 female (8474_2) and normal male (8474_1) karyotypes[61] (a generous gift from A. Amon, Massachusetts Institute of Technology; MIT, Cambridge, MA). Cells are cultured in Minimum Essential Media with 2X nonessential amino acids, 15% fetal bovine serum, 1% penicillin–streptomycin–glutamine (Invitrogen Corp., Carlsbad, CA, USA) at 37°C and 5% CO_2. DNA from large quantities of cells is purified with QIAGEN columns as recommended for cell cultures by the supplier (QIAGEN Inc, Valencia, CA). Single cells are obtained in 1ul medium using a dissecting microscope and loaded into PCR tubes. 7ul molecular biological water is added into PCR tubes, followed by adding 1μl alkaline lysis buffer [200 mM KOH and 50 mM DTT]. The samples are then incubated at 65°C for 10 min. 1ul neutralization buffer [0.9 M Tris–HCl, pH 8.3, 0.3 M KCl and 0.2 M HCl] is added to the sample to neutralize the lysis buffer[62]. The lysates are stored at -20C for future analysis.

Whole genome amplification (WGA)

Single fibroblast cells are lysed in alkaline lysis buffer as previously described [31], and processed through whole genome amplification (WGA) using the GenomePlex WGA4 kit as recommended by the supplier (Sigma Aldrich Inc). WGA DNA is purified using GenElute PCR cleanup columns (Sigma Aldrich Inc) and quantified using a Nanodrop 8000 spectrophotometer (Fisher Scientific Inc., Waltham, MA).

Next generation sequencing (NGS)

WGA DNA is normalized to 200 ng in a total volume of 35ul of molecular biological grade water (Lonza, Rockland, ME). Ion Plus Fragment Library Kit, Ion Xpress Plus Fragment Library Kit, and Ion Xpress Barcode Adapters 1-96 Kit are used to construct the WGA library as recommended by the supplier (Thermo Fisher Scientific). WGA DNA is fragmented with Ion Shear Plus reagent for 20 minutes to generate 150 to 250 base pair fragments. Fragmented DNA is then purified with Agencourt AMPure XP Reagent beads as recommended (Beckman Coulter Inc., Brea, CA). Barcoded adapter ligation and nick-repair are performed, followed by another Agencourt AMPure XP Reagent bead purification. A peak size of 270 base pairs is selected with an E‑Gel® SizeSelect™ Agarose Gel (Thermo Fisher Scientific). Size-selected DNA is amplified with 8 cycles using Platinum PCR SuperMix High Fidelity (Life Technologies). After Agencourt AMPure XP Reagent bead purification, 1ul of amplified library is assessed with D1k ScreenTape (Agilent Technologies Inc., Wilmington, DE). Individual libraries are diluted to 100picomolar with low TE buffer (Thermo Fisher Scientific). An equal amount of each of 24 samples (including four normal male control samples) is pooled together for one Ion PI Chip V2 (Thermo Fisher Scientific). Ion Sphere particles containing clonally amplified DNA are prepared with Ion PI Template OT2 200 Kit v3, and the template-positive Ion Sphere particles are then enriched with the Ion OneTouch ES (Thermo Fisher Scientific). The enriched template-positive Ion Sphere particles are sequenced with Ion PI Chip V2 and the Ion PI Sequencing 200 Kit v3 on the Ion Proton instrument (Thermo Fisher Scientific).

Data processing and Chromosomal copy number calculation

Ten bases are trimmed from the 5’ and 3’ end of each read, and the trimmed reads are aligned to

the reference Mus musculus genome (mm10) using Bowtie2 version 2.1.0 with the "sensitive-local" preset mode. The number of reads mapping to each chromosome are counted using samtools version 0.1.19, ignoring alignments with MAPQ<20.

For each sample, the normalized read count for each chromosome is calculated by dividing the raw read count of that chromosome by the average read count across all autosomes for that sample. Next, for each chromosome, the normalized read count is divided by the mean of the normalized read counts for the chromosome across all euploid male reference samples. To obtain the copy, this result is multiplied by 2 for autosomes or multiplied by 1 for sex chromosomes.

Phase II: Investigation of reciprocal errors of mice oocytes and polar bodies and incidence of aneuploidy rate from young and reproductively aged mice embryos.

Animals

In the validation study examining reciprocal chromosome segregation errors in the oocyte and polar body, sample collection will be performed at Northwestern University. CD-1 mice (Harlan Laboratories, Indianapolis, IN) of advanced reproductive age (16-19 months old) are housed in a controlled barrier facility at Northwestern University's Center of Comparative Medicine under constant temperature, humidity, and light (12h light/12h dark). Food and water are provided ad libitum. Oocytes derived from spontaneous IVM (in vitro maturation) are used for this study. Ovaries are harvested from the 8 CD-1 female mice. Cumulus-oocyte-complexes (COCs) are then collected from the oviduct. Polar bodies and oocytes are obtained and washed with Hypotonic Wash Buffer (HWB) and collected into PCR tubes for lysis, WGA, NGS and CCS analysis.

In the application study determining the incidence of aneuploidy in IVM (in vitro maturation) - and IVF-derived blastocysts, sample collection will be performed at the National Foundation for Fertility Research. CF-1 mice are obtained from Harlan Laboratories (14 females 6-9 weeks (young) and 65 females 13.5 months (aged)) and maintained on a 14:10h light:dark cycle with ad libitum access to food and water. To obtain COCs for IVM, mice are stimulated with 5 I.U. pregnant mare's serum gonadotropin (PMSG; Calbiochem, Billerica, MA) administered via injection (i.p.). Ovaries are harvested 46 to 48 h after PMSG. To obtain in vivo matured oocytes, 46 to 48 h after PMSG ovulation, mice are stimulated with 5 I.U. of human chorionic gonadotrophin (Calbiochem, Billerica, MA). COCs are collected from the oviduct 16 h later. Maturated oocytes are fertilized. Individual blastocysts are washed with HWB and placed into PCR tubes in 1 μl HWB for lysis, WGA, NGS and CCS analysis.

Ethical approval

All animal experiments were approved by the Institutional Animal Care and Use Committee (Northwestern University) or the National Foundation for Fertility Research Ethics in Research Committee, and were in accordance with National Institutes of Health Guidelines and SSR's specific guidelines and standards.

Aim 2: Evaluation of mitochondrial level

Mouse model

Experimental design

A two-phase design was implemented in the mouse study. First, to validate mouse embryonic mtDNA assessment by WGA and NGS, single-cell samples from a tumor-derived mouse cell line were tested to mimic oocyte and polar body samples, and 100-cell samples were tested to

mimic blastocysts. Cells were exposed to ethidium bromide to reduce mtDNA content. In the second phase, MtDNA levels were assessed in oocytes, polar bodies, and blastocysts. MtDNA content of blastocysts was compared between two age groups (young versus aged), different oocyte maturation methods (IVM versus IVO), and different embryo ploidy status (euploid versus aneuploid).

Cell line

A tumor-derived mouse cell line (Coriell Cell Repository ID GM05384) was cultured in Minimum Essential Media with 2X nonessential amino acids, 15% fetal bovine serum and 1% penicillin–streptomycin–glutamine (Invitrogen Corp., Carlsbad, CA, USA) at 37°C and 5% CO_2. Cultures were exposed to 25 ng/ml EtBr in full growth medium for 6 days to deplete mitochondrial DNA. Six single cell and six one hundred cell samples were picked up in 1 µl of media using a 100 µm stripper tip (Midatlantic Diagnostics, NJ, USA) under a dissecting microscope and placed into PCR tubes on day 3 and day 6. Six single cells and six one hundred cells on day 0 without EtBr exposure were picked as base line controls.

Cell lysis and WGA

Single-cell and one hundred-cell samples were lysed in alkaline lysis buffer prepared by adding 7 µl molecular biology grade water (Lonza, ME, USA) into PCR tubes, followed by 1 µl alkaline lysis buffer [200 mM KOH and 50 mM DTT]. Samples were incubated in lysis buffer at 65°C for 10 min before 1 µl of neutralization buffer [0.9 M Tris–HCl, pH 8.3, 0.3 M KCl and 0.2 M HCl] was added[63]. The lysates were stored at -20°C until the DNA was amplified by whole genome amplification (WGA) using the GenomePlex WGA4 kit as recommended by the supplier (Sigma Aldrich Inc. MO, USA). WGA DNA was purified using GenElute PCR cleanup

columns (Sigma Aldrich Inc. MO, USA) and quantified using a Nanodrop 8000 spectrophotometer (Fisher Scientific Inc., MA, USA).

Next generation sequencing (NGS)

WGA DNA was normalized to 200 ng in a total volume of 35 µl of molecular biology grade water. Ion Plus Fragment Library Kit, Ion Xpress Plus Fragment Library Kit, and Ion Xpress Barcode Adapters 1-96 Kit were used to construct the WGA library as recommended by the supplier (Thermo Fisher Scientific, CA, USA). WGA DNA was fragmented with Ion Shear Plus reagent for 20 minutes to generate 150 to 250 base pair fragments. Fragmented DNA was then purified with Agencourt AMPure XP Reagent beads as recommended (Beckman Coulter Inc., Brea, CA). Barcoded adapter ligation and nick-repair were performed, followed by another Agencourt AMPure XP Reagent bead purification. A peak size of 270 base pairs was selected with an E‑Gel® SizeSelect™ Agarose Gel (Thermo Fisher Scientific, CA, USA). Size-selected DNA was amplified with 8 cycles using Platinum PCR SuperMix High Fidelity (Life Technologies, CA, USA). After Agencourt AMPure XP Reagent bead purification, 1 µl of amplified library was assessed with D1k ScreenTape (Agilent Technologies Inc., DE. USA). Individual libraries were diluted to 100 pM with low TE buffer (Thermo Fisher Scientific, CA, USA). An equal amount of each of 24 samples was pooled together for one Ion PI Chip V2 (Thermo Fisher Scientific, CA, USA). Ion Sphere particles containing clonally amplified DNA were prepared with Ion PI Template OT2 200 Kit v3, and the template-positive Ion Sphere particles were then enriched with the Ion OneTouch ES (Thermo Fisher Scientific, CA, USA). The enriched template-positive Ion Sphere particles were sequenced with Ion PI Chip V2 and the Ion PI Sequencing 200 Kit v3 on the Ion Proton instrument (Thermo Fisher Scientific, CA, USA).

Relative mtDNA assessment

Ten bases were trimmed from both ends of each read before the reads were aligned to the *Mus musculus* nuclear and mitochondrial reference genome (mm10) using Bowtie2 version 2.1.0 with the "sensitive-local" preset mode. The number of reads mapped to each chromosome were counted using samtools version 0.1.19 while ignoring alignments with MAPQ<20. Relative mtDNA content was assessed by dividing the number of reads aligned to the mitochondrial genome (Rm) by the count of reads aligned to nuclear genome (Rn) from the same sample: $Relatvie\ mtDNA = \frac{Rm}{Rn}$. This normalization strategy removes the impact of different cell numbers from the quantitative process and is therefore a relative measure of mtDNA per cell. Then the resulting value from the blastocysts was multiplied by the correction factor F to accounts for genomic variation due to embryo gender and ploidy. $F = \frac{\sum_{n=i}(CLi*CNi)}{Euploid\ female\ total\ chromosomal\ length}$, where i is the chromosome number, CL is the chromosome length (Table 1) and CN is the chromosome copy number.

Table 1. Mouse chromosome length

Chromosome	Length (bp)
1	195,471,971
2	182,113,224
3	160,039,680
4	156,508,116
5	151,834,684
6	149,736,546
7	145,441,459
8	129,401,213
9	124,595,110
10	130,694,993
11	122,082,543
12	120,129,022
13	120,421,639
14	124,902,244
15	104,043,685
16	98,207,768
17	94,987,271
18	90,702,639
19	61,431,566
X	171,031,299
Y	91,744,698

Mouse reproductive samples

Oocyte and polar body samples were collected from a total of 8 CD-1 female mice (Harlan Laboratories, IN, USA) of advanced reproductive age (16-19 month old) at Northwestern University. Ovaries were harvested from each animal, and cumulus-oocyte-complexes (COC) were isolated from antral follicles. Cumulus cells were mechanically removed, and oocytes were cultured in a-MEM-Glutamax (Life Technologies) medium containing 3 mg/ml bovine serum albumin (MP Biomedicals, CA, USA) at 37°C in a humidified atmosphere of 5% CO_2 in air to induce spontaneous meiotic maturation. Only mature MII oocytes were used for subsequent processing. Polar bodies and mature oocytes were collected into PCR tubes for further analysis.

Blastocysts derived from IVM or IVO were collected from CF-1 mice (Harlan Laboratories, IN, USA) at Colorado Center for Reproductive Medicine. A total of 14 young females (6–9 week old) and 65 aged females (13.5 month old) were used for this application. To obtain COC for IVM, mice were stimulated with 5 IU of pregnant mare's serum gonadotropin (PMSG; Calbiochem, MA, USA). Ovaries were harvested 46 to 48 hours after PMSG injection, and COCs were recovered and subsequently matured in vitro for 18 h and then used for IVF. To obtain in vivo-matured oocytes, 46 to 48 hours after PMSG ovulation, mice were stimulated with 5 IU of human chorionic gonadotrophin (Calbiochem, CA, USA), and fully-expanded COC were collected from the oviduct 16 h later. Mature oocytes were fertilized using spermatozoa from B6D2F1 males (8 weeks old). After IVF and blastulation, Zona pellucida was removed from the embryos, and single whole blastocysts were collected into PCR tubes, followed by lysis, WGA and NGS.

Sequencing data from polar bodies, oocytes and blastocysts were analyzed for relative mtDNA content with or without normalization by the correction factor F. To investigate the possible

association of relative mtDNA level in blastocysts with ploidy status, maternal age and oocyte maturation methods, statistical analysis was carried out with ANOVA using a linear model with the natural logarithm of the mitochondrial level as the dependent variable. Independent variables include the embryo ploidy status (aneuploid versus euploid), maternal age (young versus old), and the oocyte maturation method (IVM versus IVO).

All animal experiments were approved by the Institutional Animal Care and Use Committee (Northwestern University) or Colorado Center for Reproductive Medicine Ethics in Research Committee and were carried out in accordance with National Institutes of Health Guidelines and the Society for the Study of Reproduction's specific guidelines and standards.

Human embryo study

Strategy

This study was conducted in multiple phases. First, to establish the validity of quantifying limited amounts of mitochondria from the number of cells typically obtained from a trophectoderm biopsy a cell line was used to create 5-cell samples and the results were compared to data obtained from large quantities of cells from the same cell culture. Cells were treated with ethidium bromide in order to create samples expected to possess less mitochondria as a positive control. The second phase, additional validation involved characterizing the consistency of mitochondrial DNA copy number results obtained from biological replicates of the same cell line and within the same embryo. The third phase involved characterization of DNA quantity in euploid embryos selected for transfer. By comparing mitochondrial DNA content in sibling embryos, all patient specific variables were eliminated from the evaluation of whether embryonic preimplantation mitochondrial DNA copy number was predictive of reproductive potential.

Cell line

A lymphocyte cell line (GM13118) was cultured and passaged as recommended by the supplier (Coriell Cell Repository, Camden, NJ). Ethidium bromide was added to the culture medium in order to reduce mitochondrial DNA content. Cells were obtained at multiple passages before and after treatment. In parallel, a large aliquot (>1 million cells) was obtained at the same time points for conventional DNA isolation with QIAgen columns. Results from large quantities were compared to results from 5-cell quantities.

Embryos

374 blastocysts were evaluated from patients that had undergone CCS for euploid embryo selection and a subsequent double embryo transfer in which one embryo was female and one embryo was male. Each embryo had previously undergone qPCR based CCS using a previously described protocol with preclinical validation on control cell lines, and 2 randomized controlled trials demonstrating improved outcomes. In the process of qPCR based CCS testing, excess material (one half of the preamplification reaction) not used in the procedure was made available for analysis of the mitochondrial DNA content as described below. Newborn gender and CCS based gender determination were used to determine which embryo implanted in the event of a singleton pregnancy.

Assays

Eleven different cataloged mtDNA-targeting TaqMan assays (Table 2) and a previously described custom-made AluYa5 nuclear DNA assay [16] were used to perform preamplification (multiplex PCR) of the leftover PCR product (Figure 1A). Each 50ul reaction consisted of 25ul of the left over PCR reaction, 12.5ul of 0.2X of each TaqMan assay, and 25ul of 2X TaqMan

PreAmp Master Mix and was run for 18 cycles as recommended by the supplier (Thermo Fisher Scientific). Subsequent qPCR was performed with each assay run in quadruplicate 5ul reactions with 1ul of the mtDNA preamp reaction, 0.25ul of each TaqMan assay (20X), and 2.5ul of TaqMan Gene Expression Master Mix. Standard TaqMan PCR settings were used and real-time data was collected on an ABI 7900 Instrument. Individual mtDNA assays that result in more variable assay cycle threshold (C_T) measurements as compared to other assays are recursively eliminated until there was a set of 3 assays that have highly consistent results across hundreds of samples (Figure 1B). These 3 most robust assays (ATP6, Hs02596862_g1; ND6, Hs02596879_g1; and RNR1, Hs02596859_g1) are used for measuring the mitochondrial level of samples in the current study. Each assay is carried out 4 times for each sample in final experiments.

Table 2. List of TaqMan® Assays

Assay ID	Target	Gene ID	Gene	Transcript Characteristics
Hs02596879_g1	Mitochondrial encoded gene	4541	MT-ND6	OXPHOS complex I
Hs02596873_s1	Mitochondrial encoded gene	4535	MT-ND1	OXPHOS complex I
Hs02596862_g1	Mitochondrial encoded gene	4508	MT-ATP6	OXPHOS complex V
Hs02596867_s1	Mitochondrial encoded gene	4519	MT-CYB	OXPHOS complex III
Hs02596878_g1	Mitochondrial encoded gene	4540	MT-ND5	OXPHOS complex I
Hs02596864_g1	Mitochondrial encoded gene	4512	MT-CO1	OXPHOS complex IV
Hs02596861_s1	Mitochondrial encoded gene	MT-D-loop	MT-7S	
Hs02596863_g1	Mitochondrial encoded gene	4509	MT-ATP8	OXPHOS complex V
Hs02596877_g1	Mitochondrial encoded gene	4539	MT-ND4L	OXPHOS complex I
Hs02596859_g1	Mitochondrial encoded gene	4549	MT-RNR1	
Hs02596874_g1	Mitochondrial encoded gene	4536	MT-ND2	OXPHOS complex I
AIHR17K	Nuclear encoded gene		AluY5a	Endogenous control

Eleven different TaqMan assays targeting mtDNA and a custom-made TaqMan assays targeting nuclear AluYa5 gene were used to analyze relative mtDNA amount.

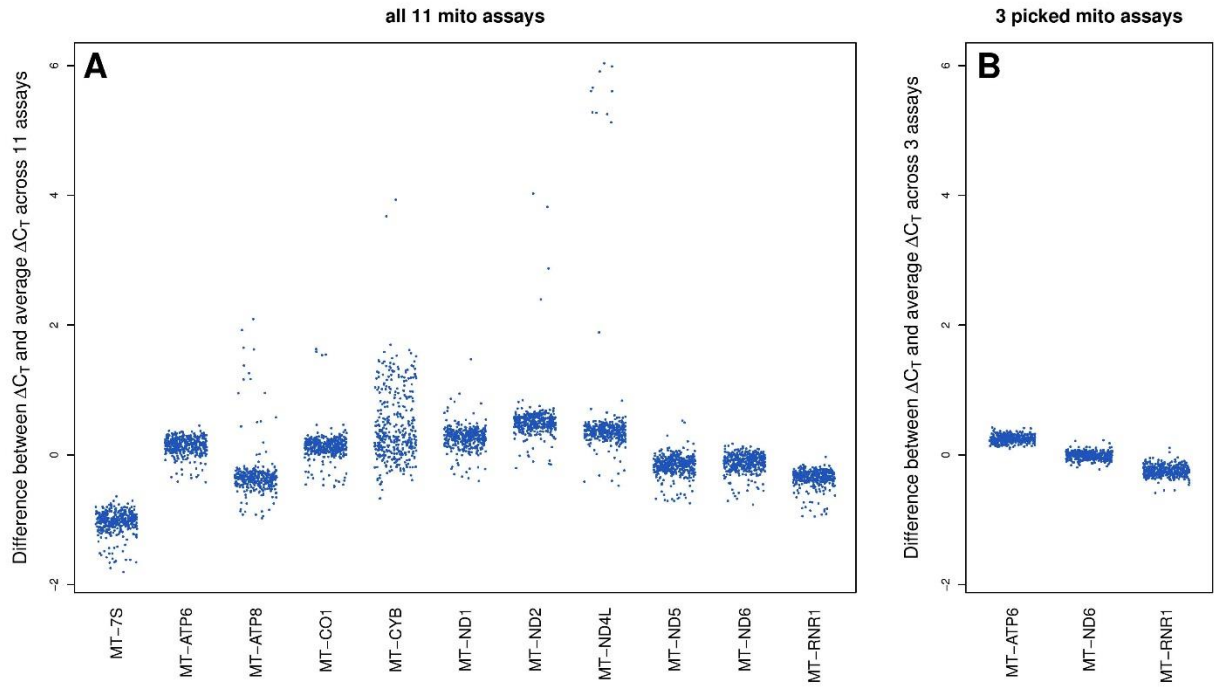

Figure 1. Selection of mitochondrial TaqMan assays. Some assays yield results that are sometimes inconsistent with other assays (A). Such assays are recursively eliminated until there is a set of 3 most robust assays for the quantitation of mtDNA level (B).

Data Analysis

For relative quantitation of mtDNA of a sample, the median C_T value for the 4 measurements for each individual assay is calculated first, followed by the calculation of a ΔC_T between each mtDNA assay and the reference AluY5a assay. Relative mtDNA quantity is defined as the additive inverse of the average ΔC_T for the 3 mtDNA assays.

In the first phase of the study, multiple replicates using 5-cell samples were processed and compared with a large aliquot of cells (>1 million cells) at the time points described above in order to validate the assay for use on limited quantities of mitochondria. Subsequently, ΔC_T values from replicates were averaged and compared with ΔC_T values from the large aliquot at each time point.

Embryo relative mtDNA quantity was evaluated in order to assess putative associations with reproductive success and other cycle parameters. First, nested logistic regression models were utilized to test if ΔC_T values predicted overall embryo outcome (implanted and delivered vs failed). A subset analysis was performed including only the 69 DETs where one of the two sibling embryos successfully implanted and delivered. To test for a difference in relative mtDNA level between the successful and failed embryos within each pair, a one-sided (lower mtDNA levels with better pregnancy outcome) paired t-test on the average ΔC_T was carried out for the 69 pairs of embryos with single births. Lastly, utilizing simple linear models, other parameters such as oocyte maternal age, embryo biopsy day, and embryo morphology were tested for correlations with mtDNA quantity.

All data collection and analysis was approved by the IRB. Subjects provided written consent for use of these samples in research.

Aim 3: Characterization of endometrial microbial environment

Control samples for platform validation

Single colonies of three different bacterial strains (Table 3) were picked from the LB agar plates and inoculated into the tube with liquid LB. The bacterial cultures were incubated at 37°C for 12-18 hours in a shaking incubator with loosened caps. The growth of the bacteria was measured by OD600. The DNA was isolated from an aliquot of each culture (Procedure for DNA isolation is needed).

Artificial mixture of the culture and DNA were prepared to validate that polymicrobial samples can be identified by the NGS based method. 1ul of each 1:1000 diluted culture including the mixtures was loaded into PCR tubes. 7ul molecular biological water was added into PCR tubes, followed by adding 1μl alkaline lysis buffer [200 mM KOH and 50 mM DTT]. The samples were then incubated at 65°C for 10 min. 1ul neutralization buffer [0.9 M Tris–HCl, pH 8.3, 0.3 M KCl and 0.2 M HCl] was added to the sample to neutralize the lysis buffer. 1ng of DNA including the mixtures was normalized in 10ul molecular biological grade water.

Ion 16S Metagenomics workflow (Thermo Fisher Scientific)

Ion 16S Metagenomics workflow analyzes seven out of nine hypervariable regions of 16S rRNA gene. Hypervariable regions 2, 3, 4, 6, 7, 8 and 9 are amplified as individual 200~300 bp fragments in one of two multiplex PCR reactions (Primer A and B) (Figure 2, Thermo Fisher Scientific).

Table 3. Ten samples from three different bacterial strains for validation; Negative control is included

Sample	Strain	Type
C1	*Escherichia coli*	culture
C2	*Staphylococcus epidermidis*	culture
C3	*Cyanobacterium Synechococcus* sp. IU 625	culture
D1	*Escherichia coli*	genomic DNA
D2	*Staphylococcus epidermidis*	genomic DNA
D3	*Cyanobacterium Synechococcus* sp. IU 625	genomic DNA
MC1	Mixed	culture
MC2	Mixed	culture
MD1	Mixed	genomic DNA
MD2	Mixed	genomic DNA
NTC	None	negative control

Validation samples including NTC were amplified by the two multiplex primer pools. After purification with Agencourt AMPure XP Reagent beads (Beckman Coulter Inc., Brea, CA), 1ul of amplified DNA was assessed with D1k ScreenTape (Agilent Technologies Inc., Wilmington, DE). Equal amounts of the purified V2-4-8 and V3-67–9 amplification reactions were combined for each sample. 100ng of each pooled sample was used for the library preparation by using Ion Xpress Plus Fragment Library Kit, and Ion Xpress Barcode Adapters 1-96 Kit (Thermo Fisher Scientific). The ends of the amplicons were repaired to generate blunt ends, followed by Agencourt AMPure XP Reagent beads purification. Barcoded adapter ligation and nick-repair were performed, followed by another Agencourt AMPure XP Reagent bead purification. Adaptors and Barcodes ligated DNA was amplified with 8 cycles using Platinum PCR SuperMix High Fidelity (Life Technologies). After Agencourt AMPure XP Reagent bead purification, 1ul of amplified library was assessed with D1k ScreenTape (Agilent Technologies Inc., Wilmington, DE). Individual libraries were diluted to 100pM with low TE buffer (Thermo Fisher Scientific). An equal amount of each of the 15 validation samples was pooled together as the final library for sequencing on one Ion 318 Chip V2 (Thermo Fisher Scientific). Ion Sphere particles containing clonally amplified DNA was prepared with Ion PGM Hi-Q Template OT2 Kit, and the template-positive Ion Sphere particles were then enriched with the Ion OneTouch ES (Thermo Fisher Scientific). The enriched template-positive Ion Sphere particles were sequenced with Ion Chip 318 V2 and the Ion PGM Hi-Q Sequencing Kit on the Ion PGM instrument (Thermo Fisher Scientific) (Figure 5). Data was uploaded into Ion Reporter TM software version 4.4 to perform 16S Metagenomics beta workflows.

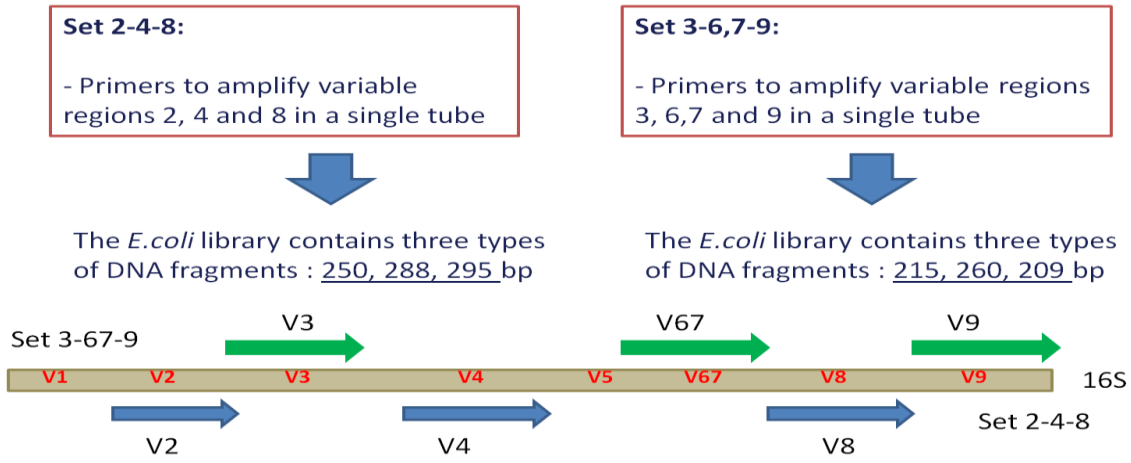

Figure 2. Two sets of primers pools are used to amplify 7 of the 9 hypervariable regions of the 16S rDNA gene in bacteria: (Thermo Fisher Scientific)

• Pool A: Primer set to amplify V2-4-8 • Pool B: Primer set to amplify V3-6,7-9

Illumina 16S V3-V4 and V4 workflow

The target sequences used in Illumina 16S workflow are the 16S V3-V4 region and V4 region only. The library preparation of this workflow involves a two-step, tailed amplicon approach. The locus-specific primers contain sequence tails that allow a second PCR to add Nextera XT indexed adapters. Fusion primers increase melting point, efficiency, and specificity while avoiding the disadvantages of long primers, such as hairpins, self-dimers, primer dimers and chimreas (Illumina).

10ul of the validation samples including NTC were amplified with 0.2uM forward and reverse primers and 25ul 2X TaqMan Preamplification Master Mix (Thermo Fisher Scientific) in 50ul reactions. PCR cycling conditions were set to 10 min at 95°C followed by 18 cycles of 15 sec at 95°C and 4 min at 60°C on Applied Biosystems 2720 thermocycler. 7.5ul of preamplified DNA was used to set up the first PCR with 0.2uM forward and reverse primers (Table 4) and 12.5 ul 2X Kapa HiFi HotStart ReadyMix (KapaBiosystems) in 25ul reactions. The PCR cycling conditions were 3 min at 95°C, 25 cycles of 30 sec at 95°C, 30 sec at 55°C and 30 sec at 72°C, followed by 5 min at 72°C on Applied Biosystems 2720 thermocycler.

The amplified DNA was purified with Agencourt AMPure XP Reagent beads. The second PCR was set up to add indexes to the amplified DNA by adding 5ul of purified DNA to 25ul 2X Kapa HiFi HotStart ReadyMix, 5ul Nextera XT Index 1 and 2 primers (FC-121-1002, Illumina) in 50ul reactions. Each sample must have a unique combination of indexes. The reaction was set at 3 min at 95°C, 8 cycles of 30 sec at 95°C, 30 sec at 55°C and 30 sec at 72°C, followed by 5 min at 72°C on Applied Biosystems 2720 thermocycler, followed by another Agencourt AMPure XP Reagent beads purification.

Table 4. Illumina 16S workflow V3V4 and V4 primers

Primer	Sequence (5’-3’)
16S V3V4 Amplicon PCR Forward Primer	TCGTCGGCAGCGTCAGATGTGTATAAGAGACAGCCTACGGGNGGCWGCAG
16S V3V4 Amplicon PCR Reverse Primer	GTCTCGTGGGCTCGGAGATGTGTATAAGAGACAGGACTACHVGGGTATCTAATCC
16S V4 Amplicon PCR Forward Primer	TCGTCGGCAGCGTCAGATGTGTATAAGAGACAGAYTGGGYDTAAAGNG
16S V4 Amplicon PCR Reverse Primer	GTCTCGTGGGCTCGGAGATGTGTATAAGAGACAGTACNVGGGTATCTAATCC

16S V3V4 amplicon is about 430 bps, and 16S V4 amplicon is about 210 bps after amplification with the primer pairs.

1ul of library DNA was access with D1k ScreenTape (Agilent Technologies Inc., Wilmington, DE). Individual libraries were diluted to 4nM with resuspension buffer (Illumina). An equal amount of each of the 15 validation samples was pooled together as the final library. The final loading concentration of 4pM was used for sequencing on one MiSeq v3 reagent kit (Illumina) using paired 300bp reads. The Metagenomics Workflow performed a build in taxonomic classification using the Greengenes database and showed genus or species level classification in a graphical format.

Customized Data analysis

Ion 16S Metagenomics

For each amplicon region, sequence reads were assigned to OTUs with modified 16S Metagenomics beta workflows in Ion Reporter TM software version 4.4. OTU clustering was performed with the UCLUST on the QIIME package. Taxonomy assignments of these OTUs based on the Greengenes database were carried out using the RDP classifier version 2.2 within the QIIME package.

Illumina 16S Metagenomics

Paired-end sequencing from Illlumina MiSeq platform produced two separate read files, called SE1 for the first read, and SE2 for the second. Poor quality nucleotides at the 5' ends were trimmed for both SE1 and SE2 until a reliable base quality score (above 33) was reached. Ea-utils Fastq-mcf was used to identify and trim primer sequences, filter reads without primer sequence, and trim nucleotides with poor quality at the 3' ends. The V4 amplicon is ~240 base pairs. To generate about 100bp overlap between SE1 and SE2, the V4 reads were shortened to 180bp. The filtered and trimmed SE1 and SE2 reads are then joined by overlapping read-pairs together using Ea-utils

Fastq-join. The joined sequences with improper length for V3-V4 (~470bp) and V4 (~240bp) amplicons are filtered out. The fastq files with correct read length were then converted to fasta files for further analysis using the QIIME package. Chimera sequences were identified with the USEARCH 6.1 on QIIME and removed by the QIIME package. OTU clustering was performed with the UCLUST on the QIIME package. Taxonomy assignments of these OTUs based on the Greengenes database were carried out using the RDP classifier version 2.2 within the QIIME package.

Validation on genomic DNA mixture of 20 bacterial strains on Illumina 16S V4 workflow

Microbial Mock Community B was obtained through BEI Resources, NIAID, NIH as part of the Human Microbiome Project: Genomic DNA from Microbial Mock Community B (Even, Low Concentration), v5.1L, for 16S RNA Gene Sequencing, HM-782D

The genomic DNA was amplified by V4 primers. Library was prepared and sequenced on one MiSeq v3 reagent kit (Illumina) by using paired 300bp reads as previously described. Taxonomy assignments were performed to identify the bacterial strains.

Control samples for establishing sensitivity

Single colonies of four different bacterial strains including two Gram-positive and two Gram-negative bacteria (Table 5) were picked from the LB agar plates and inoculated into the tube with liquid LB broth. The bacterial cultures were incubated at 37°C for 6-10 hours in a shaking incubator with loosened caps until the OD_{600nm} reached 0.6. The bacterial gDNA was isolated from an aliquot of each culture using bacterial genomic DNA isolation kit following manufacturer's recommendation (Norgen Biotek Corp, ON, Canada). Artificial mixtures of the culture and gDNA were prepared to validate that poly-microbial samples can be identified by this NGS based method.

A ten-fold serial dilution was performed on single- and poly-microbial cultures (Table 6). 1 µl of each diluted culture including the mixtures was loaded into PCR tubes. 7 µl molecular biology water (Lonza, ME, USA) was added into PCR tubes, followed by adding 1 µl alkaline lysis buffer [200 mM KOH and 50 mM DTT]. The samples were then incubated at 65°C for 10 min. 1 µl neutralization buffer [0.9 M Tris–HCl, pH 8.3, 0.3 M KCl and 0.2 M HCl] was added to the sample to neutralize the lysis buffer. 1 ng of DNA including the mixtures was normalized in 10 µl molecular biology water (Lonza, ME, USA).

Characterizing the microbiome at the time of embryo transfer on Illumina 16S V4 workflow

The patients underwent in vitro fertilization cycle using standard protocol. Embryo transfer was performed with a Wallace Classic soft tip catheter (Smiths Medical, Dublin, OH, USA) with the formable outer sheath advanced under ultrasound guidance. All patient samples were collected under approval from the Internal Review Board (IRB). After embryo transfer, the distal 5mm portion of the transfer catheter tip was placed in a PCR tube. Lysis, amplification, library preparation, sequencing and taxonomy assignment were performed as previously described. The Shannon Diversity Index (SDI), total OTU counts, and fraction of reads were compared utilizing generalized linear models.

Table 5. Single- or poly-microbial samples from four different bacterial strains for validation; Negative control is included.

Strain	Gram Staining	Type
Escherichia coli	negative	culture
Proteus vulgaris	negative	culture
Staphylococcus epidermidis	positive	culture
Bacillus cereus	positive	culture
Mixed		culture
Escherichia coli	negative	gDNA
Proteus vulgaris	negative	gDNA
Staphylococcus epidermidis	positive	gDNA
Bacillus cereus	positive	gDNA
Mixed		gDNA

The validation study included two Gram-positive and two Gram-negative bacteria. Cultures with different cell number were lysed directly to establish the sensitivity of the methodology, and the gDNA isolated from a large amount of cells was served as control. Artificial mixtures represented the poly-microbial samples.

Table 6. A ten-fold serial dilution on single and poly-microbial cultures.

No. Of serial dilution	Estimated Cell Number/ul
0	$6X10^5$
1	$6X10^4$
2	$6X10^3$
3	$6X10^2$
4	$6X10^1$
5	$6X10^0$

There were 6 serial dilutions of the bacterial culture. The highest dilutions contained about 6 cells in the lysates.

Results

Aim 1: Establishment of CCS for mouse model

Phase I: NGS based CCS successfully identifies aneuploidy in single mouse cells

Two mouse embryonic fibroblasts with trisomy 16 female (8474_2) and normal male (8474_1) karyotypes were used for validation. Genomic DNA from large quantities of cells was purified. Single cell lysates were amplified by WGA and the concentration was measured using a Nanodrop 8000 spectrophotometer (Figure 3A). The libraries of Genomic DNA and single cell WGA DNA for NGS were constructed (Figure 3B). For the normal male cell line (8474_1), in both Genomic DNA and single cell WGA DNA, the copy number for all autosomes was two, but the sex chromosomes (X and Y) each had a copy number of one (Figure 4A and 4B). For the trisomy 16 female cell line, the presence of the extra copy of chromosome 16, two copies of chromosome X, and zero copies of chromosome Y were detected in both Genomic DNA and single cell WGA DNA , as expected (Figure 4C and 4D). These findings validated the application of CCS using WGA and NGS to individual mouse somatic cells.

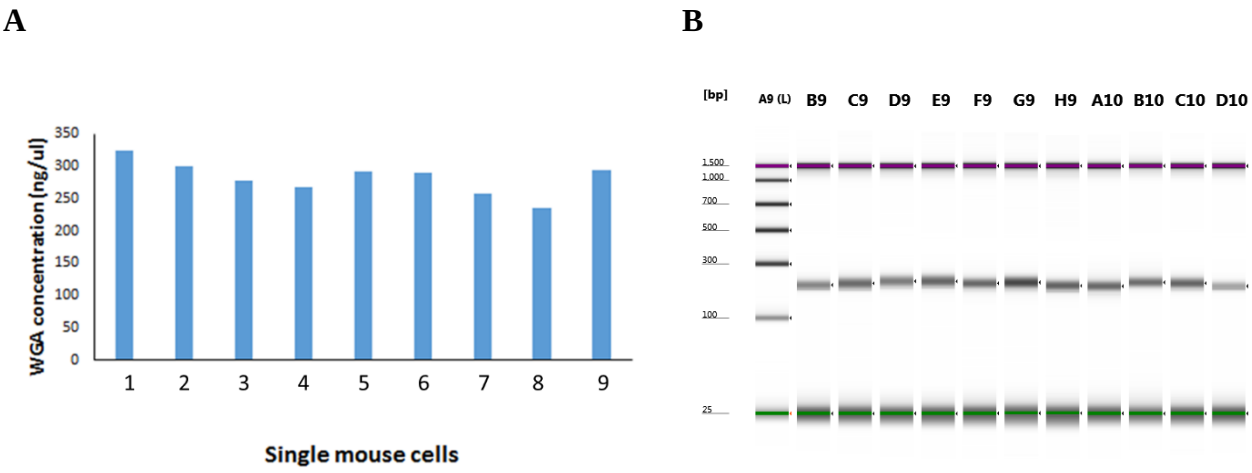

Figure 3. Amplification and library construction of single cells

A) Single cell lysates were amplified by WGA with concentration ~282 ± 25 ng/ul.

B) The libraries of Genomic DNA and single cell WGA DNA.

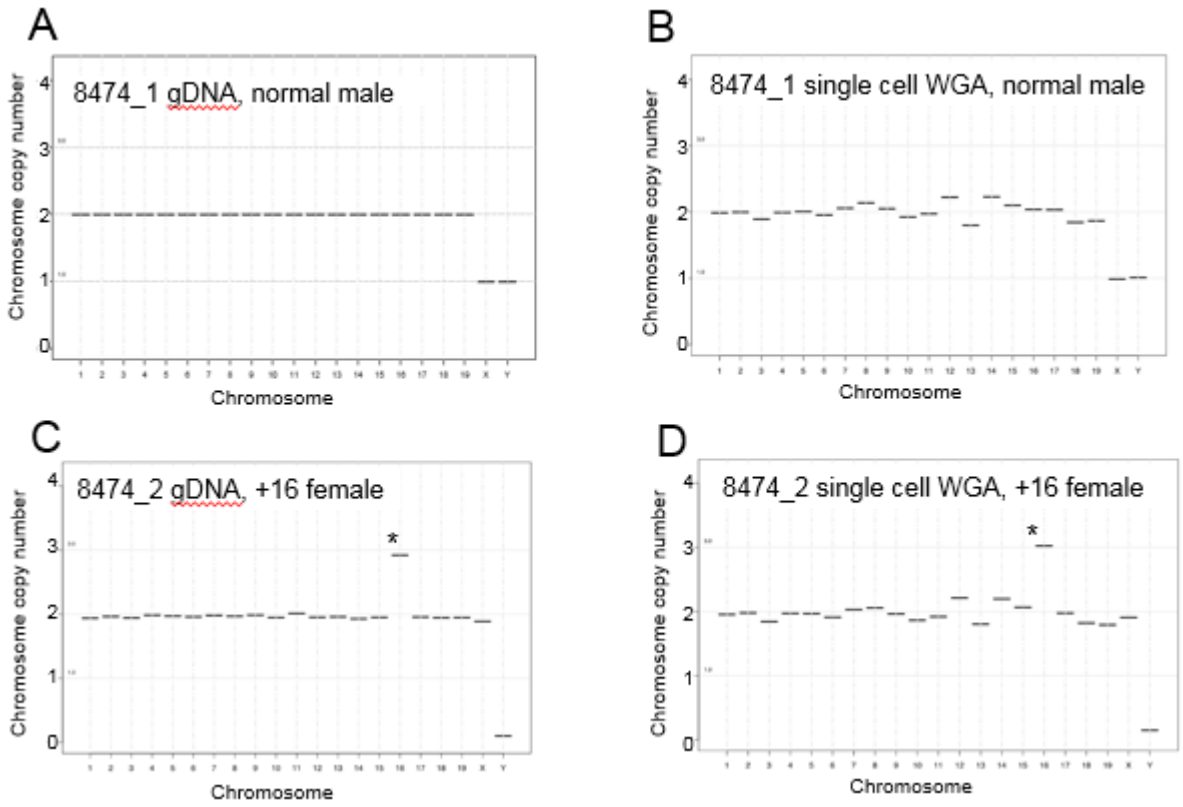

Figure 4. NGS was used to identify the karyotype of mouse cells of known ploidy. Copy number plots of genomic DNA isolated from pooled cells(A) and single cell WGA DNA (B) for normal male mouse embryonic fibroblasts (8474_1) showed one copy of chromosome X and Y is detected. Copy number plots of genomic DNA isolated from pooled cells(C) and single cell WGA DNA (D) for trisomy 16 female mouse embryonic fibroblasts (8474_2) showed three copies of chromosome 16 were detected.

Phase II: Investigation of reciprocal errors of mice oocytes and polar bodies and incidence of aneuploidy rate from young and reproductively aged mice embryos.

NGS-based CCS successfully detects reciprocal errors in polar bodies and oocytes

An average of 15 ± 3 oocytes from 8 individual CD-1 mice ranging in age from 15-19 months. Following IVM, an average of 80% (range 57%-96%) of oocytes from these reproductively aged mice were able to resume meiosis and reach MII. The oocyte was separated from the first polar body and then performed WGA and NGS using these matched cells (Figure 5, A and B). 40 matched oocytes and first bodies were analyzed, representing a subset of 2–8 oocytes per mouse. Interpretable sequencing data were obtained from 37 of 40 oocytes and 35 of 40 polar bodies (Table 7). The remaining sequencing data from the oocytes (3 of 40) and polar bodies (5 of 40) were considered chaotic due to the noise level in the observed copy number assignment patterns. Such patterns could potentially reflect complex aneuploidy, biological mosaicism, sample degradation, or methodological artifacts (Table 7 and Figure 6). Because we were unable to distinguish among these possibilities, we considered these data nonresults, unless we were able to obtain clear sequencing results from the reciprocal polar body or gamete (Table 8). As expected, euploid mouse oocytes and their matched polar bodies had a copy number of 2 for all nineteen autosomes and the X chromosome but a copy number of zero for the Y chromosome (Figure 53, C and D). Any copy number pattern that differed from this was considered aneuploid. In the subset of 40 oocytes that were sequenced, we observed an overall aneuploidy incidence of 15% (6 of 40 oocytes) and a euploidy incidence of 85% (34 of 40 oocytes) (Table 8). From an individual animal standpoint, 6 of 8 mice had aneuploid oocytes, with an incidence ranging from 13% to 20%, whereas 2 mice did not (Table 8).

In the 6 aneuploid oocytes, we identified chromosome segregation errors in seven different autosomes: 2, 5, 7, 9, 11, 12, and 15 (Table 8). In five of the oocytes, the aneuploidy was attributed to premature separation of sister chromatids (PSSC). This was evident as a reciprocal gain or loss of a single chromatid, or a copy number of three or one for a particular chromosome(s), in the respective matched oocyte and polar body samples (Table 8 and Figure 7, A and B, chromosomes 2, 5, 7, 11, 12, and 15). In one oocyte, we identified nondisjunction of chromosome 9 homologs that resulted in a copy number of 4 in the polar body and a reciprocal copy number of zero in the oocyte (Table 8 and Figure 7, C and D). In the majority of the aneuploid oocytes (5 of 6), we detected the mis-segregation of a single chromosome/chromatid. However, in one oocyte, we identified PSSC of two chromosomes, 11 and 12 (Table 8 and Figure 7, E and F). Taken together, these results demonstrate that NGS-based CCS is a reliable and quantitative tool with which to identify chromosome- specific aneuploidy and the type of mis-segregation in the mouse oocyte.

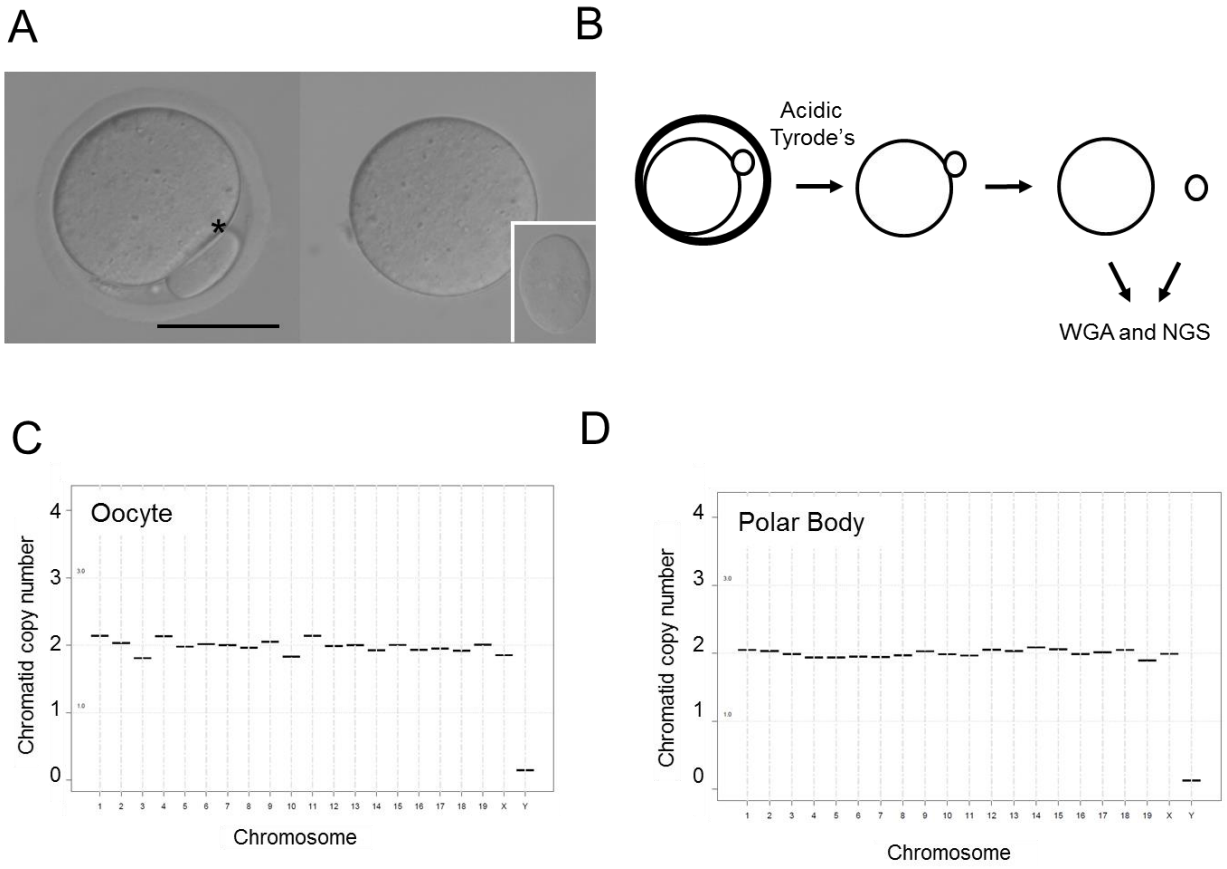

Figure 5. Use of WGA and NGS for chromosome assessment in individual matched polar bodies and occytess is shown. A) MII oocytes with visible polar bodies were used for sequencing analysis. A representative image is shown in the left panel (*polar body). The oocyte and polar body were separated from each other following removal of the zona pellucida. The matched oocyte and polar body (inset) are shown in the right panel following separation. Bar ¼ 50 lm. B) Schematic shows the experimental workflow. The zona pellucida was removed from each MII oocyte using acidic Tyrode solution, the matched polar body and oocyte were gently separated by aspiration and WGA, and NGS was performed in each cell. Representative sequencing plots of a euploid oocyte (C) and its matched polar body (D) are shown. Note, all autosomes and the X chromosome have a copy number of 2, whereas the Y chromosome has a copy number of 0.

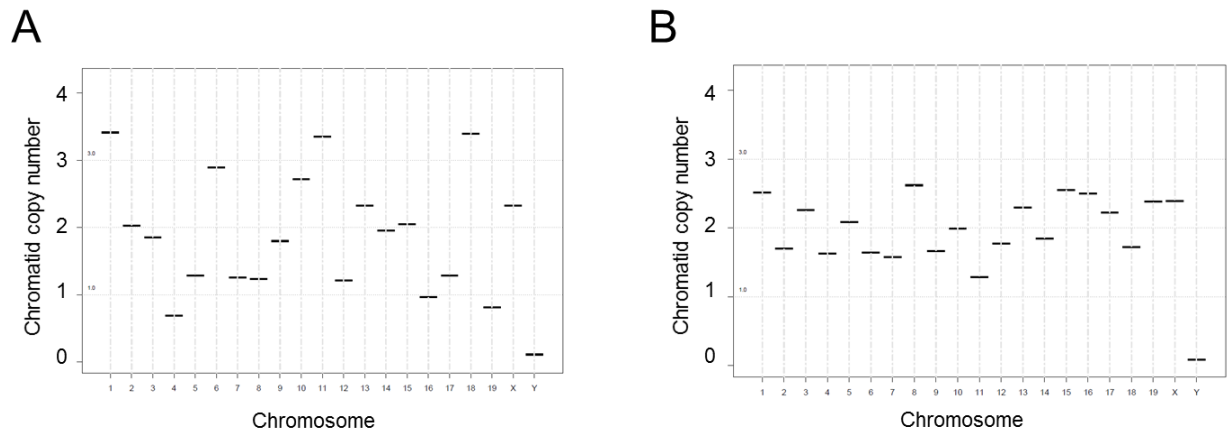

Figure 6. Examples of chaotic sequencing results. Representative sequencing plots of chaotic reads obtained from an individual (A) oocyte and (B) polar body. These chaotic reads were observed infrequently and only in the oocyte and polar body samples.

Reprinted from *Biology of Reproduction Volume 94, Issue 4, Article 76, 1-11, Treff NR, Krisher RL, Tao X, Garnsey H, Bohrer C, Silva E, Landis J, Taylor D, Scott RT, Woodruff TK, Duncan FE. Next Generation Sequencing-Based Comprehensive Chromosome Screening in Mouse Polar Bodies, Oocytes, and Embryos. Copyright (2016), with permission from Oxford University Press, License Number 4123790372109*

Table 7. Summary of Chaotic Egg Reads

Animal ID	Egg # chaotic/total (%)	PB # chaotic/total (%)
A	0/5 (0%)	1/5 (20%)
B	0/5 (0%)	1/5 (20%)
C	2/5 (40%)	0/5 (0%)
D	0/5 (0%)	0/5 (0%)
E	0/8 (0%)	2/8 (25%)
F	0/2 (0%)	0/2 (0%)
G	0/5 (0%)	0/5 (0%)
H	1/5 (20%)	1/5 (20%)
Total	3/40 (8%)	5/40 (13%)

Chaotic results were detected only in the oocytes and polar bodies, which could be caused by complex aneuploidy, sample degradation, or methodology artifacts.

Table 8. Summary of Egg Aneuploidy

Animal ID	# Aneuploid eggs/total (%)	Egg Aneuploidy	Reciprocal PB Aneuploidy
A	1/5 (20%)	+11, -12	-11, +12
B	1/5 (20%)	--9	++9
C	1/5 (20%)	chaotic	-5
D	0/5 (0%)	N/A	N/A
E	1/8 (13%)	+15	-15
F	0/2 (0%)	N/A	N/A
G	1/5 (20%)	+7	-7
H	1/5 (20%)	chaotic	+2

The overall aneuploidy rate was 15%. Five aneuploidies were caused by MI PSSC and one was caused by MI non-disjunction.

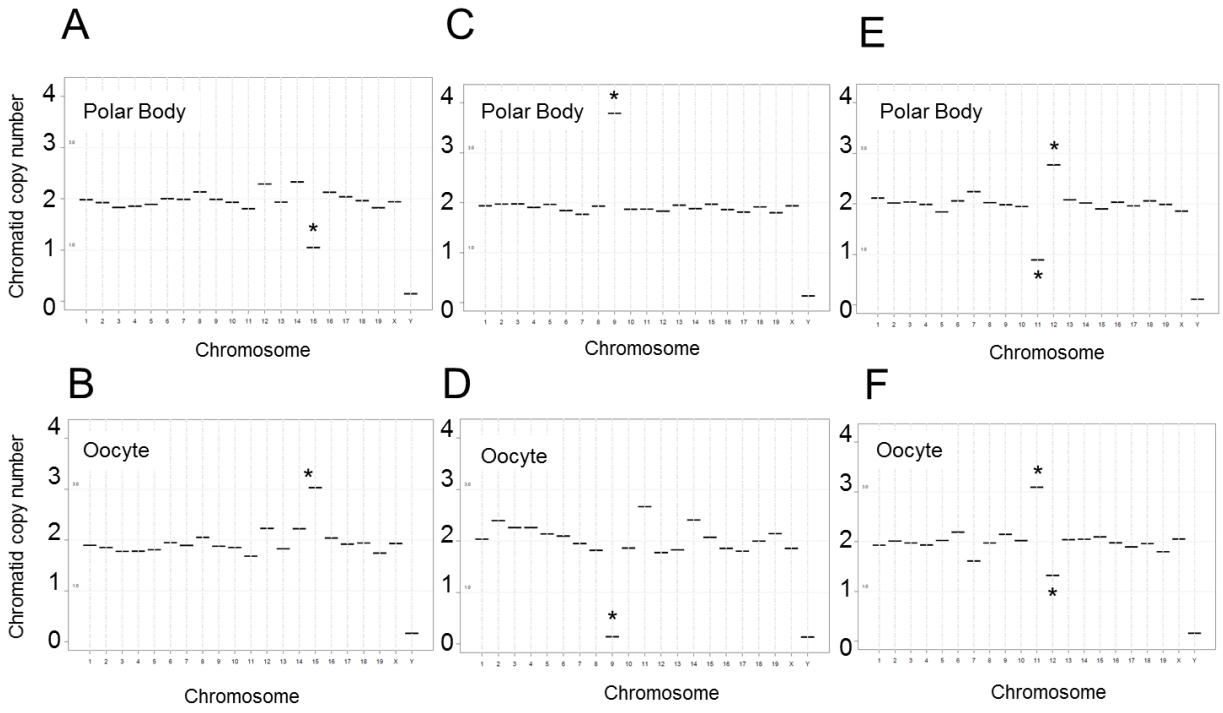

Figure 7. Detection of reciprocal aneuploidies in metaphase II oocytes and matched polar bodies. Sequencing plots from matched polar bodies (A, C, and E) and oocytes (B, D, and F) that reveal reciprocal aneuploidies, including premature separation of sister chromatids (loss/gain of 1 copy of chromosome 15 [A and B]) non-disjunction of homologs (loss/gain of 2 copies of chromosome 9 [C and D]), and complex aneuploidy (loss/gain of 1 copy of chromosomes 11 and 12 [E and F]). *Chromosomes with an abnormal copy number indicative of aneuploidy.

NGS Based CCS Successfully Identifies Aneuploidy in mouse reproductive samples

We next applied our NGS based CCS technology for aneuploidy detection in individual preimplantation mouse blastocysts produced via IVM or IVO from reproductively young and aged females (Figure 8). Importantly, our analysis was done on intact blastocysts, which precludes detection of mitotic errors. Thus, the aneuploidy we determined with this particular approach was limited to meiotic errors.

In young animals more COC were collected per female. A total of 199 and 89 COC were collected from 5 (39.8 COC/female) and 9 (9.9 COC/female) mice after IVO and IVM, respectively. 56.1% of fertilized IVM oocytes and 56.4% of fertilized IVO oocytes from young females developed to blastocyst. A subset of 33 IVM blastocysts from young females was analyzed by CCS; WGA was successful in 32 of them. Forty-six percent of the embryos were male. Aneuploidy in three blastocysts was detected (9.4%) (Table 9), with mis-segregation of single chromosomes (chromosomes 2 and 13) (Table 10). WGA was successful in 27 of 29 IVO embryos examined; 15% of the embryos were male. Only one blastocyst was aneuploid (3.7%, Table 9), with a segregation error in chromosome 8 (Table 10).

In contrast to reproductively young mice, aged mice had fewer morphologically healthy COCs to be used for IVM, fewer ovulated COCs following IVO, and an increased incidence of aneuploidy compared to younger counterparts, despite successful fertilization and blastocyst development. For aged IVM oocytes, 223 COC were obtained from a total of 55 CF1 mice age 13.5 months (4.1 COC/female). Following IVF and embryo culture, 75.8% of the fertilized eggs reached the blastocyst stage (160/211). A subset of 50 blastocysts was analyzed, and WGA was successful in 47 cases. Six of 47 blastocysts were aneuploid (12.8%) (Table 9), with segregation errors involving chromosomes 7, 8, 9, 12, 13, 15, 16, 18, and 19 (Table 10). Twenty-eight of 47

embryos were male (59.6%); 5 of the 6 aneuploid embryos had aneuploidy of a single chromosome (Table 10). For aged IVO oocytes, 10 CF1 females age 13.5 months were used to obtain 106 COC (10.6 COC/female), of which 72.7% of fertilized oocytes reached the blastocyst stage (64/88). A subset of 67 IVM blastocysts was submitted for chromosomal analysis, and WGA was successful in 65 cases. Twenty of the 65 embryos (30.8%) were aneuploid (Table 9), with segregation errors involving multiple chromosomes (Table 10). Thirteen of the 20 aneuploid embryos possessed aneuploidy of a single chromosome, whereas the remaining embryos each had 2, 4, or 6 different chromosomes that contributed to aneuploidy (Table 10).

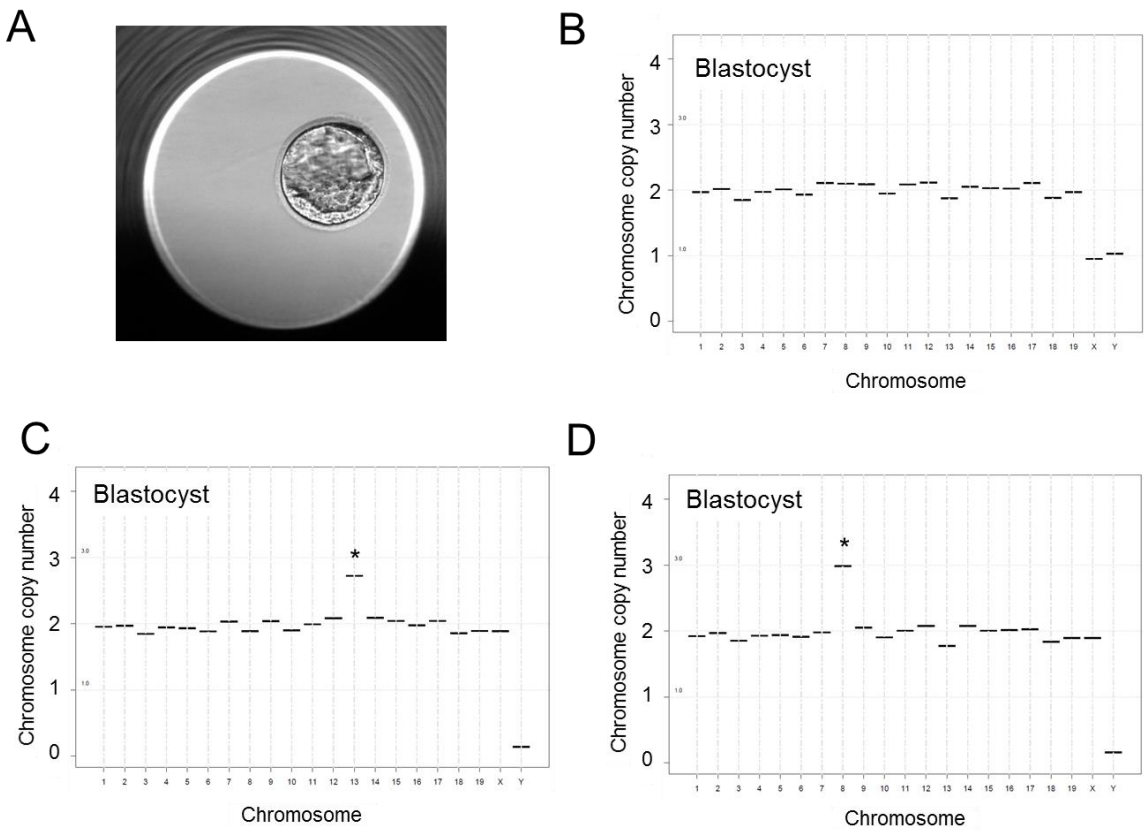

Figure 8. Use of WGA and NGS for chromosome assessment in individual blastocysts originating from young and reproductively aged female. A) Blastocysts derived after IVM and IVF were used for sequencing. A representative blastocyst is shown. Representative sequencing plots of euploid (B) and aneuploid blastocysts (C and D) are shown. Aneuploidy is due to a gain of 1 copy of chromosome 13 (C) and a gain of 1 copy of chromosome 8 (D). *Chromosomes with an abnormal copy number indicative of aneuploidy.

Table 9. Summary of embryo aneuploidy

Age group	Maturation	Aneuploid	Euploid	Total	No result	% Aneuploidy
Young	IVO	1	26	27	2	3.7[a]
	IVM	3	29	32	1	9.4[a]
Aged	IVO	6	41	47	3	12.8[a]
	IVM	20	45	65	2	30.8[b]

[a,b] Groups with different superscripts are statistically different from each other (P<0.05)

The aneuploid rate from old mice was higher than young mice with both oocyte maturation methods (IVO and IVM). The frequency of aneuploidy observed in IVM-derived blastocysts was higher than IVO-derived blastocysts in both age groups.

Table 10. Description of embryo aneuploidy

Group	Maturation	Embryo ID	Aneuploidy	Sex
Aged	IVM	1	+1, +5, +8, +13	Female
Aged	IVM	2	+3, -14, -17, +19	Male
Aged	IVM	3	+16	Female
Aged	IVM	4	+19	Male
Aged	IVM	5	-12	Female
Aged	IVM	6	+2	Male
Aged	IVM	7	+8	Female
Aged	IVM	8	+3	Male
Aged	IVM	9	+3, +10	Female
Aged	IVM	10	+13	Female
Aged	IVM	11	+15	Male
Aged	IVM	12	-19	Male
Aged	IVM	13	+10,+12	Male
Aged	IVM	14	+7,+11	Male
Aged	IVM	15	-9,+19	Female
Aged	IVM	16	-3	Female
Aged	IVM	17	-4	Female
Aged	IVM	18	-3,+11,+14,+19	Male
Aged	IVM	19	+12	Female
Aged	IVM	20	+1	Male
Aged	IVO	21	+13	Male
Aged	IVO	22	+8	Female
Aged	IVO	23	+19	Male
Aged	IVO	24	+15	Male
Aged	IVO	25	+7,-9,+12,+15,+16,+18	Female
Aged	IVO	26	-13	Female
Young	IVM	27	+2	Female
Young	IVM	28	+13	Male
Young	IVM	29	+13	Female
Young	IVO	30	+8	Female

Aim 2: Evaluation of mitochondrial level

Mouse model

Reliability analysis of mtDNA content on cultured cells

Relative mtDNA levels were assessed in six single- and 100-cell samples following day 0, day 3, and day 6 treatment with EtBr. Exposure to EtBr for three and six days resulted in a decrease in relative mtDNA levels in both the single and 100-cell samples as expected (Figure 9). The standard deviation of six single cell samples was higher than that samples containing 100 cells,as would be expected based on the variation between different single cells.

Assessment of mtDNA content in mouse reproductive samples

The mtDNA level was determined and compared for 40 oocytes and their corresponding polar bodies as well as 171 blastocysts (Fig 10). Polar bodies contained an average of 0.9% of mtDNA relative to oocytes due to asymmetric segregation of cytoplasmic content during meiosis. Oocytes contained 180-fold higher mtDNA content compared to the cells in blastocysts. This is consistent with current understanding of the timing of mitochondrial biogenesis during early development: mitochondria accumulate in the oocyte during oogenesis and reaches a peak in the fully grown oocyte. There is little mitochondrial biogenesis and mtDNA replication and mitochondria are split into daughter cells in post-fertilization cell division during preimplantation development[18], and there is much less mtDNA in the blastocyst cells compared to oocytes.

Analysis of mtDNA content in mouse blastocysts

A total of 171 blastocysts in which CCS results had been obtained were analyzed for the relative mtDNA content with or without normalization by the correction factor F. In the young age

group: 27 IVO blastocyst were analyzed, and 1 was aneuploid; 32 IVM blastocysts were analyzed, and 3 of them were aneuploid. In the old age group: 47 IVO blastocysts were assessed, 6 of them were aneuploid; 65 IVM blastocysts were assessed, 20 of them were aneuploid (Table 3). In both one-way ANOVA and multiple factor ANOVA with interaction terms (model log(mtDNA.level) = ploidy.status + age.group + oocyte.maturation.method + ploidy.status:age.group + age.group:oocyte.maturation.method + oocyte.maturation.method:ploidy.status), embryo ploidy status, maternal age group, and oocyte maturation method were all found to be associated with embryo mtDNA level (Before F factor correction: one way ANOVA p-values were 0.0045, 4.5e-7, and 0.0052, respectively; After F factor correction: p-values were 0.0006, 2.0e-6, and 0.0001, respectively). Cell in aneuploid blastocysts contained higher quantity of mtDNA compared to euploid blastocysts (Figure 11A and 11B). Younger age was associated with lower relative mtDNA level (Figure 11C and 11D). And IVO treatment for oocyte maturation was associated with higher relative mitochondrial level (Figure 11E and 11F).

Table 11. Total of 171 blastocysts with CCS results

Age group	Oocyte maturation	Aneuploid	Euploid	Total
Young	IVO	1	26	27
	IVM	3	29	32
Old	IVO	6	41	47
	IVM	20	45	65

171 blastocysts with CCS results were analyzed for mtDNA level. The relative mtDNA content of blastocysts were compared between different ploidy status (euploid versus aneuploid), distinct age groups (young versus aged), and different oocyte maturation methods (IVM versus IVO)

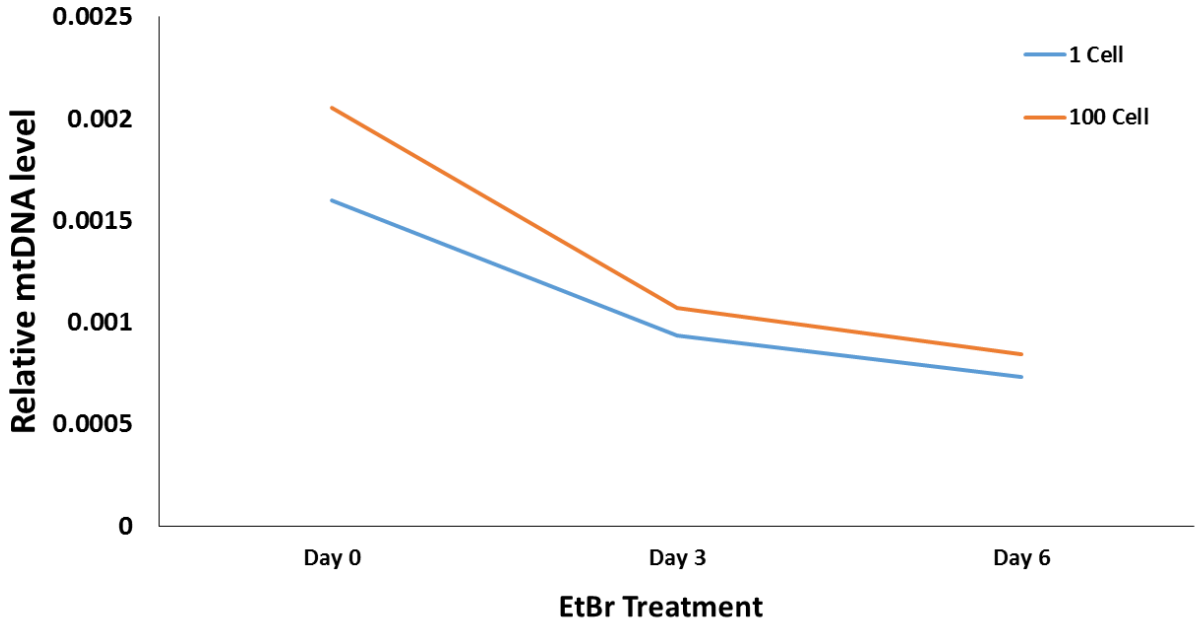

Fig 9. Reltive mtDNA content in single- and 100-cell samples with EtBr treatment. Six single- and 100- cell samples were collected with EtBr exposure for 0, 3, and 6 days. EtBr treatment impairs the mtDNA replication, therefore, mtDNA content decreased in single- and 100-cell samples with longer exposure to EtBr as expected.

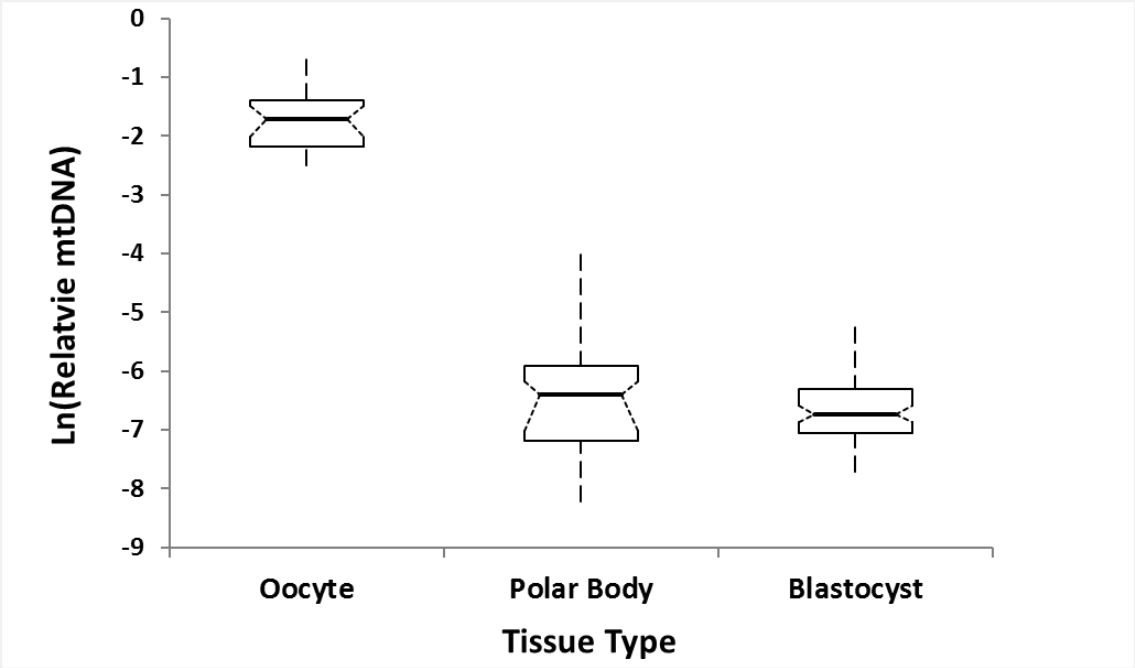

Fig 10. Box plots for relative mtDNA content level in mouse reproductive samples. Y-axis represented the nature logarithmic scale of relative mtDNA level. Relative mtDNA level from 40 oocytes had a median of 0.18, 40 polar body had a median of 0.0017, and 171 blastocyst had a median of 0.001.

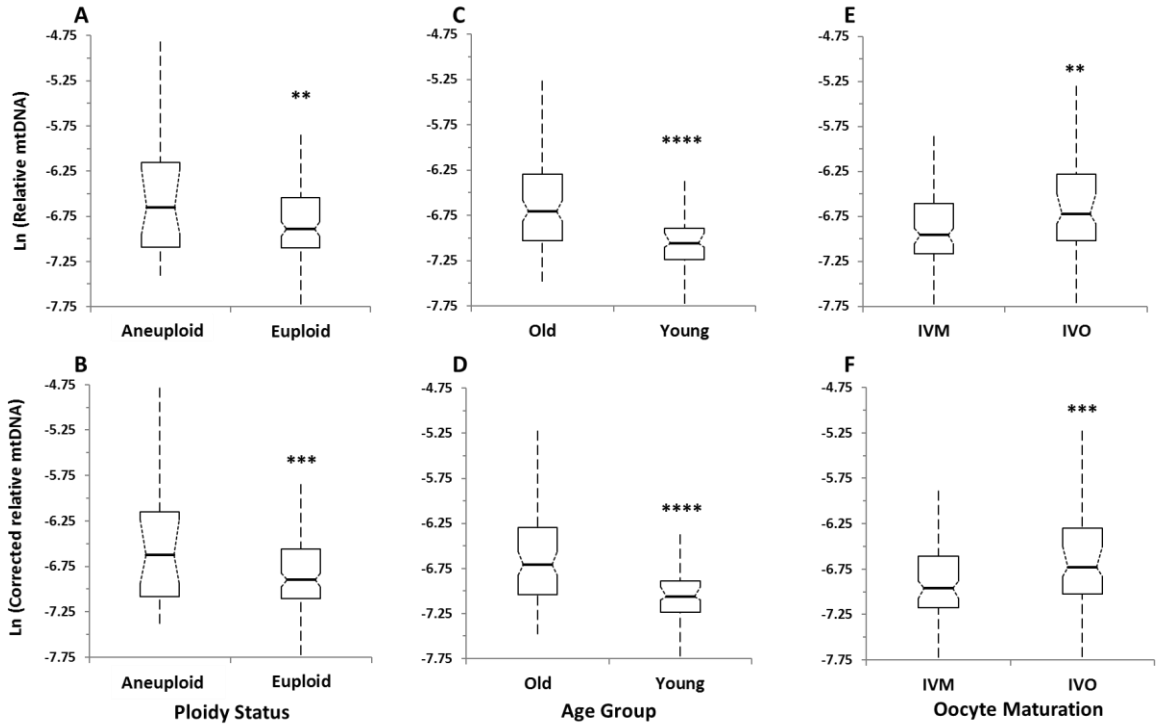

Figure 11. Box plots for relative mtDNA content in mouse blastocysts. Y-axis represented the nature logarithmic of relative mtDNA level. NGS analysis of 171 blastocysts showed a statistically significant increase () in aneuploidy blastocytes before (A) (P = 0.0045) and after F factor correction (B) (P = 0.0006). Cells in blastocysts from old mice contained a significantly higher level of mtDNA before (C) (P = 4.5e-7) and after F factor correction (D) (P = 2.0e-6). NGS analysis also showed cells in blastocysts derived from IVO contained a significantly higher amount of mtDNA compared to IVM before (E) (P = 0.0052) and after F factor correction (F) (P = 0.0001).

Human embryo study

Assay Development

Accurate quantitation of mtDNA was achieved with qPCR using 3 mitochondrial-specific primers and an AluY5a assay for normalization. Using a cell line treated with ethidium bromide to reduce mitochondria content, large aliquots of cells were evaluated for relative mitochondrial copy number and processed. As expected, ΔC_T values increased from Day 0 to Day 6 indicating a decreasing mitochondrial copy number (Figure 12). In order to evaluate the assay's performance using limited amounts of DNA resembling excess material available from clinical specimens, 5-cell samples were subsequently evaluated in a similar fashion. Samples processed in replicates of six resulted in consistent results and likewise had increasing ΔC_T values signifying decreasing copies of mtDNA.

Clinical Outcomes

A total of 374 embryos utilized in 187 DETs (one embryo of each gender per transfer) were available for analysis. Of these, 69 (36.9%) resulted in the live birth of a singleton, 84 (44.9%) resulted in multiple births, and 34 (18.2%) failed to result in any birth. Association testing was carried out to identify if mtDNA quantity predicted overall pregnancy success (Figure 13A). Analysis of the entire cohort of 374 embryos did not identify a significant association between relative mtDNA quantity and embryo outcome ($p=0.488$ when maternal age is included as a covariate).

In order to eliminate patient-specific variables from the evaluation of whether embryonic preimplantation mitochondrial content was predictive of reproductive potential, the 69 DETs resulting in singleton delivery were subsequently analyzed separately. Since a male and a female

embryo were always transferred together, offspring gender was used to distinguish the implanted embryo from the non-implanted one allowing a powerful and well-controlled assessment of reproductive potential. Relative mtDNA quantity from embryos that implanted and delivered versus those that did not were compared (Figure 13 B,C,D). A paired t-test showed that mtDNA levels were not predictive of a successful outcome ($p=0.402$ for a one-sided test).

Additional clinical and embryological parameters were also evaluated for associations with mitochondrial copy number (Figure 14). Relative mtDNA content for each of the 374 embryos was evaluated for correlations with the following parameters: maternal age at time of retrieval, embryo biopsy day, and embryo morphology. Mitochondrial copy number decreased with increasing age ($p=0.00020$). Embryos biopsied on day 5 were more likely to have higher quantities of mtDNA compared with those biopsied on day 6 ($p=7.2 \times 10^{-21}$). Embryo morphology was evaluated per practice routine using a grading system based on assessment of certain characteristics such as expansion, inner cell mass (ICM) quality and trophectoderm quality. Blastocyst expansion was graded from 1 to 6 with the latter representing a fully hatched embryo. Trophoblast and ICM were graded as A, B, or C with grade A representing good quality and grade C representing poor quality. Superior blastocyst expansion was correlated with lower mitochondrial content ($p=2.3 \times 10^{-23}$). Higher quality trophoblast and ICM were similarly correlated with lower mitochondrial quantity ($p=0.00040$ and $p=0.0010$, respectively).

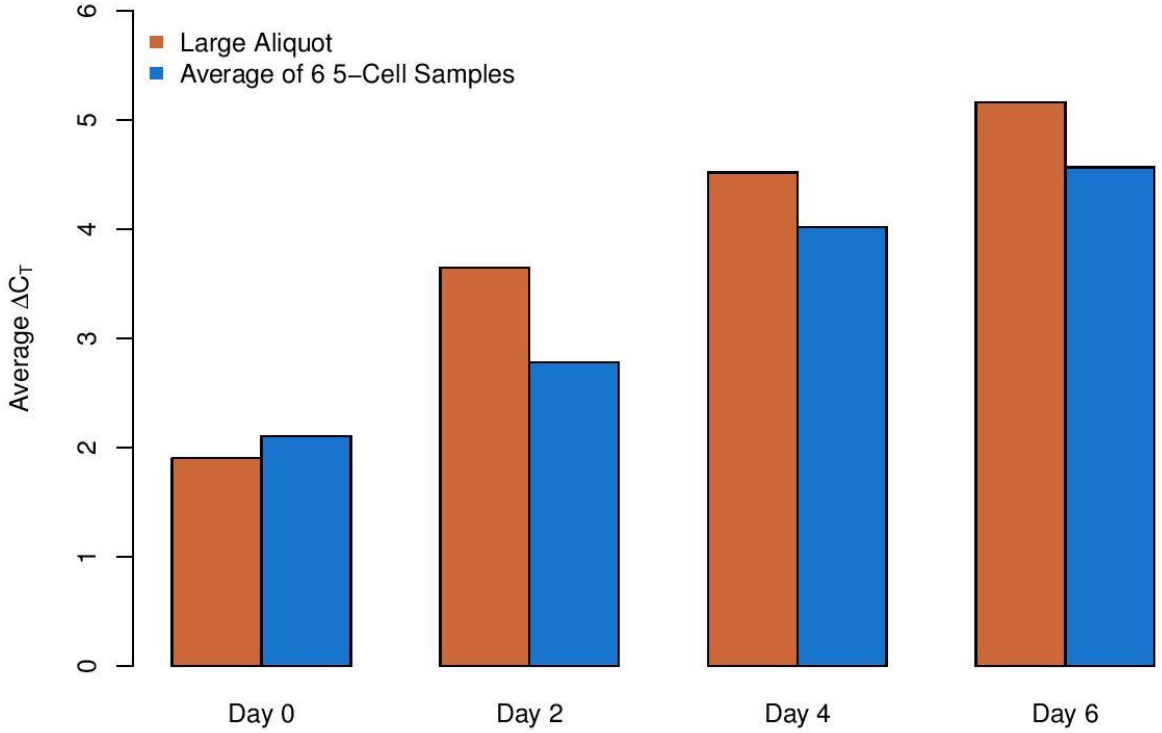

Figure 12. Average ΔC_T values for 5-cell and large aliquot samples using cell lines exposed to ethidium bromide for 0, 2, 4, and 6 days

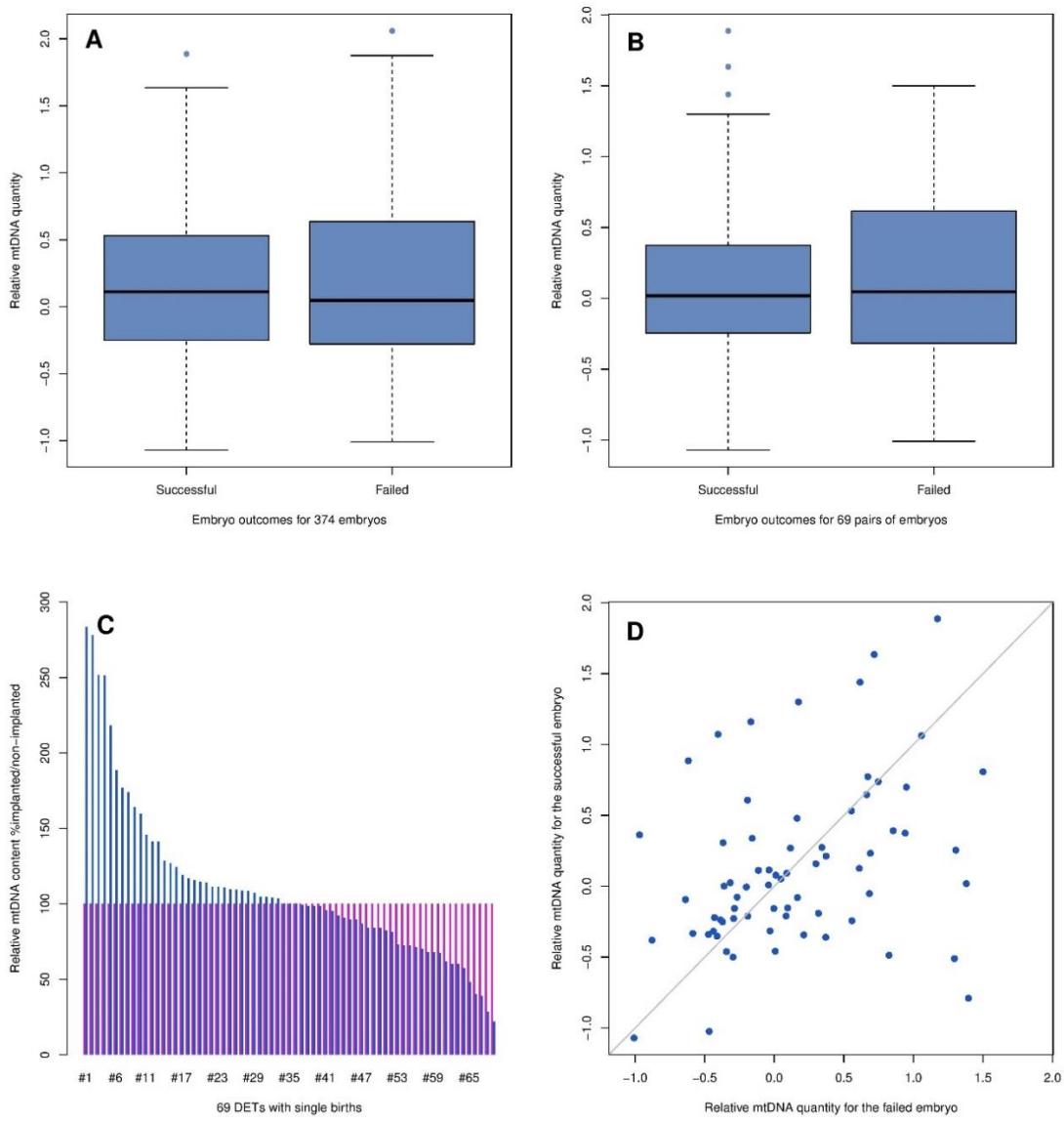

Figure 13. Relative mtDNA quantity versus pregnancy success. A. Relative mtDNA quantity stratified by embryo pregnancy success status for all 374 embryos in the current study; B. Relative mtDNA quantity stratified by embryo pregnancy success status for the 69 pairs of embryos used in DET that resulted in single births; C. Relative mtDNA quantity ratio between each of the 69 pairs of embryos used in DET that resulted in single births. Blue bars indicate the ratios between two embryos within each pair; D. Comparison of the relative mtDNA quantity for the successful versus failed embryo for each of the 69 pairs. The identify line is shown in gray.

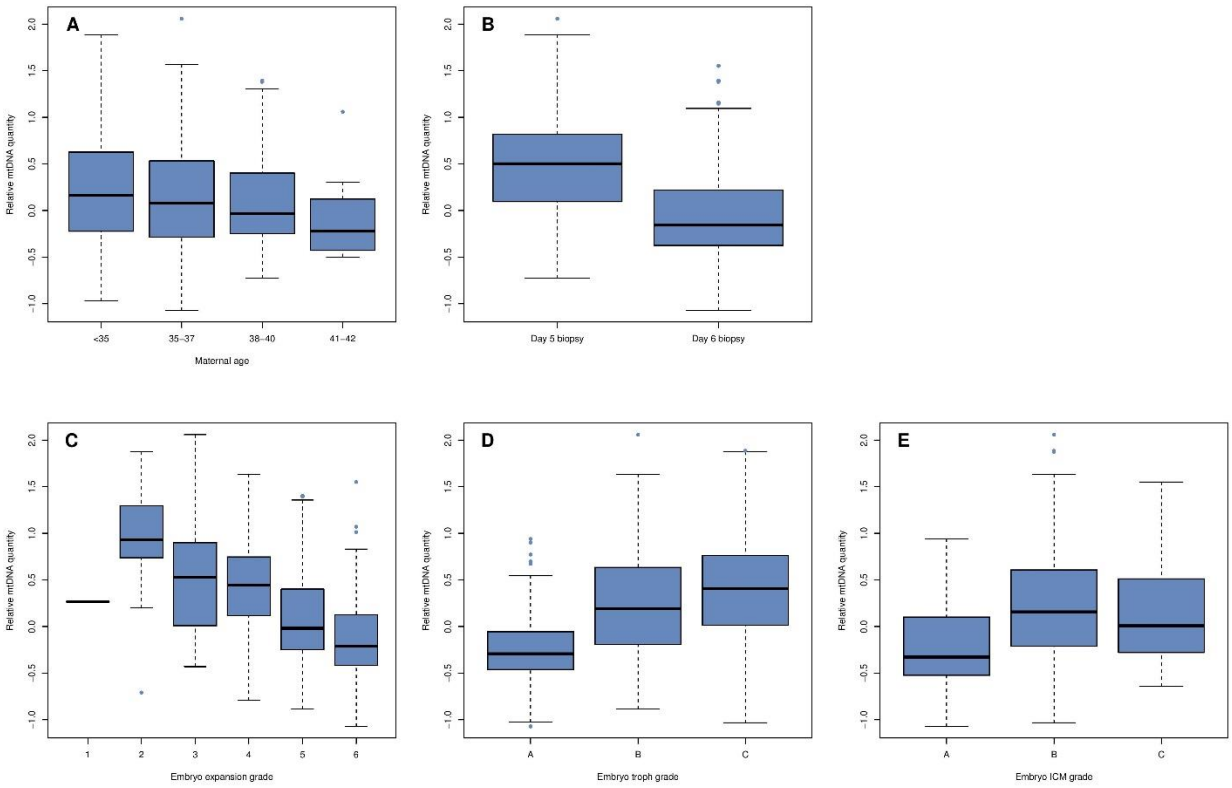

Figure 14. Association of secondary clinical parameters with mitochondrial quantity.

A. Relative mtDNA quantity stratified by maternal age group; B. mitochondrial quantity in biopsy samples stratified by biopsy day; C.-E. mitochondrial quantity in biopsy samples stratified by embryo expansion stage, trophectoderm grading, and ICM grading, respectively.

Aim 3: Characterization of endometrial microbial environment

Ion 16S Metagenomics workflow

Ion Reporter™ Software enabled the identification of microbes present in complex polybacterial samples by using both curated GreenGenes and curated MicroSeq® ID 16S reference databases (Figure 15). Ion 16S metagenomics workflow detected family level for all of the samples. However, only two single organism samples were detected at the genus level. The mixed samples showed consistent results with single organism samples (Figure 16). Our lowest target is the identification of genus level, so the customized data analysis was performed to improve the taxonomic assignment.

Illumina 16S V3-V4 and V4 workflow

MiSeq build-in Metagenomics Workflow performed a taxonomic classification using the Greengenes database. Table 12 showed the example data of taxonomic assignment of V3-V4 and V4 from sample C1 (*Escherichia coli* Culture). For both V3-V4 and V4 amplicons, over 70% of the reads were assigned to the genus level, but the species level did not match the known strain. The genus level assignment had been improved for all the other samples through Illumina 16S Metagenomics Workflow.

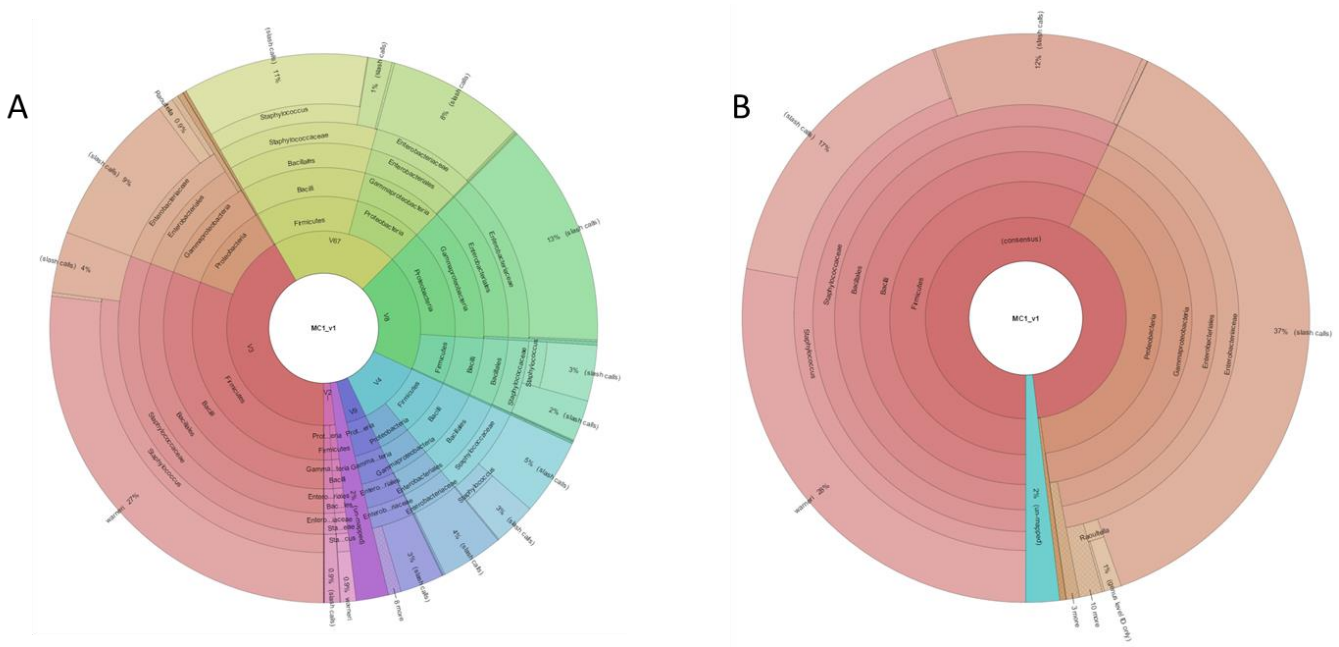

Figure 15. Example of data visualization with Krona charts from sample MC1 (Artificial mixture of three bacterial culture) A) Visualizing results by primers. B) Consensus view of sample MC1.

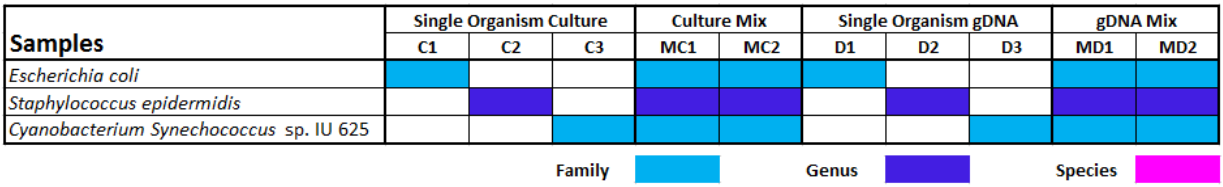

Figure 16. Identification in single and polymicrobial samples from Ion 16S metagenomics workflow. Only two organism samples C2 and D2were detected at the genus level and all other single organism samples were detected at the family level. The mixed samples were consistent with the single organism samples.

Table 12. Taxonomic classification from V3V4 and V4 of sample C1 (*Escherichia coli* Culture) using MiSeq build-in Metagenomics Workflow.

Amplicon: V3V4

Kingdom	Phylum	Class	Oder	Family	Genus	Species	num hits	% hits
Unclassified							48502	7.285
Bacteria	Proteobacteria	Gammaproteobacteria	Enterobacteriales	Enterobacteriaceae	Escherichia	albertii	443155	66.559
Bacteria	Proteobacteria	Gammaproteobacteria	Enterobacteriales	Enterobacteriaceae			83008	12.467
Bacteria	Proteobacteria	Gammaproteobacteria	Enterobacteriales	Enterobacteriaceae	Seratia	Entomophia	61745	9.274
Bacteria	Proteobacteria	Gammaproteobacteria	Enterobacteriales	Enterobacteriaceae	Escherichia		17009	2.555
Bacteria	Proteobacteria	Gammaproteobacteria	Enterobacteriales	Enterobacteriaceae	Enterbacter		12390	1.861

Amplicon: V4

Kingdom	Phylum	Class	Oder	Family	Genus	Species	num hits	% hits
Unclassified							49600	8.315
Bacteria	Proteobacteria	Gammaproteobacteria	Enterobacteriales	Enterobacteriaceae	Seratia	Entomophia	278481	46.687
Bacteria	Proteobacteria	Gammaproteobacteria	Enterobacteriales	Enterobacteriaceae	Escherichia	albertii	151214	25.351
Bacteria	Proteobacteria	Gammaproteobacteria	Enterobacteriales	Enterobacteriaceae	Escherichia		56149	9.413
Bacteria	Proteobacteria	Gammaproteobacteria	Enterobacteriales	Enterobacteriaceae			41106	6.891
Bacteria	Proteobacteria	Gammaproteobacteria	Enterobacteriales	Enterobacteriaceae	Seratia		10706	1.795
Bacteria	Proteobacteria	Betaproteobacteria	Burkholderiales	Oxalobacteraceae	Ralstonia	insidiosa	9233	1.548

Customized Data analysis

Ion 16S Metagenomics

Our customized analysis improved the results. ~37% reads of C1 (*Escherichia coli* Culture) were assigned to the species level, and 1% reads were assigned to the genus level, but the majority reads are still at the family level (Figure 17). All the other single and polymicrobial samples showed the similar improvement.

It was found that there were variations of read counts among the seven hypervariable regions in the same samples (Figure 18). C3 showed dominant amplification of V3 region. However, MD1 and MD2 contained the genomic DNA of the five strains, but there was no amplification of V9, which was amplified in D1. The bias of amplification caused the problem of quantitative analysis of the microbiome.

Illumina 16S V3-V4 and V4 workflow

The customized data analysis was performed to identify the taxonomy of the samples. After the quality control and joining steps, V3-V4 had over 70% of reads filtered out for each sample, but V4 only had ~10% failed reads. V3-V4 was longer than V4 and the error frequency of the sequencing increased with longer reaction. Moreover, the overlap sequence for joining of V3-V4 was shorter than V4, which made the overlapping more difficult (Figure 19). Taxonomic assignments of these OTUs based on the Greengenes database were carried out using the RDP classifier version 2.2 within the QIIME package. Figure 21 showed accurate species identification of V3V4 and V4 for sample C1 (*Escherichia coli* Culture). V4 (Figure 20B) had higher OUT counts than V3V4 (Figure 20A). For both amplicons V3-V4 and V4, the genus or species level were identified in the single and polymicrobial samples (Figure 21).

Figure 17. Customized taxonomic assignment of C1 (*Escherichia coli* Culture). Over 60% reads are assigned to family level.

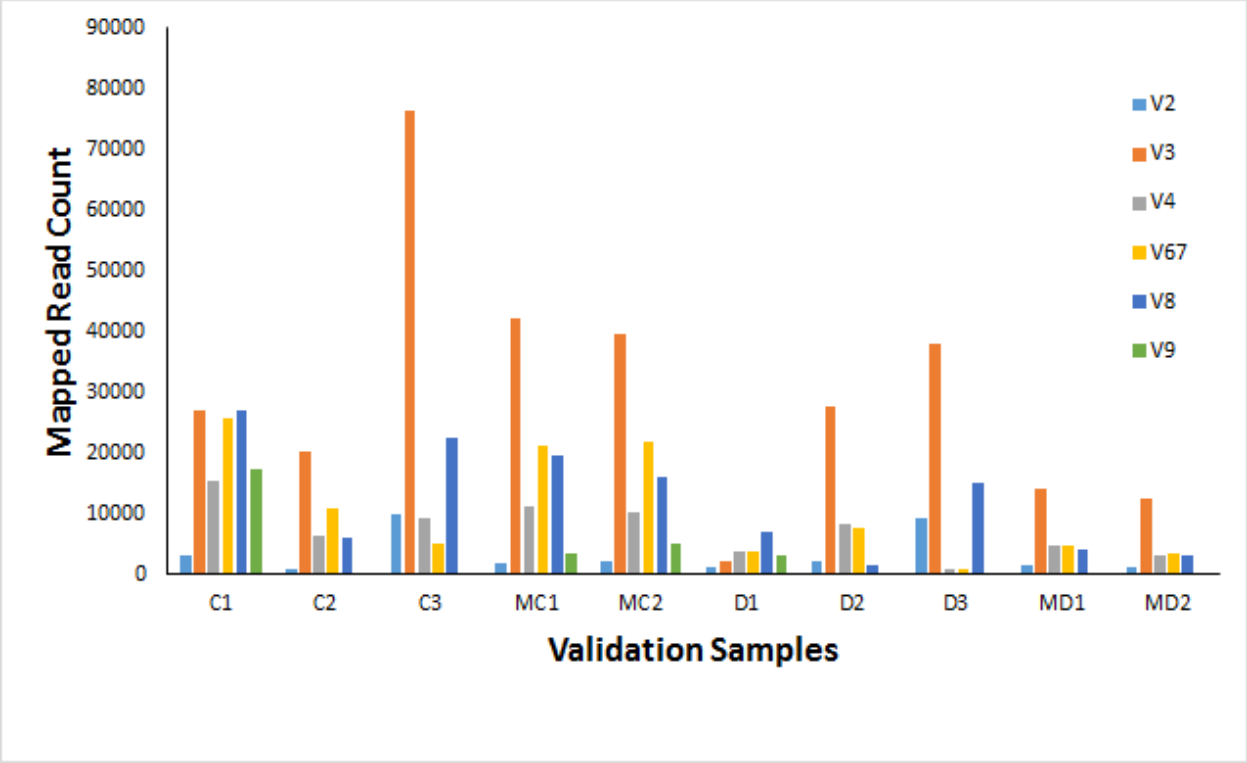

Figure 18. The mapped counts of seven individual hypervariable regions for validation samples. There is amplification variation among these regions.

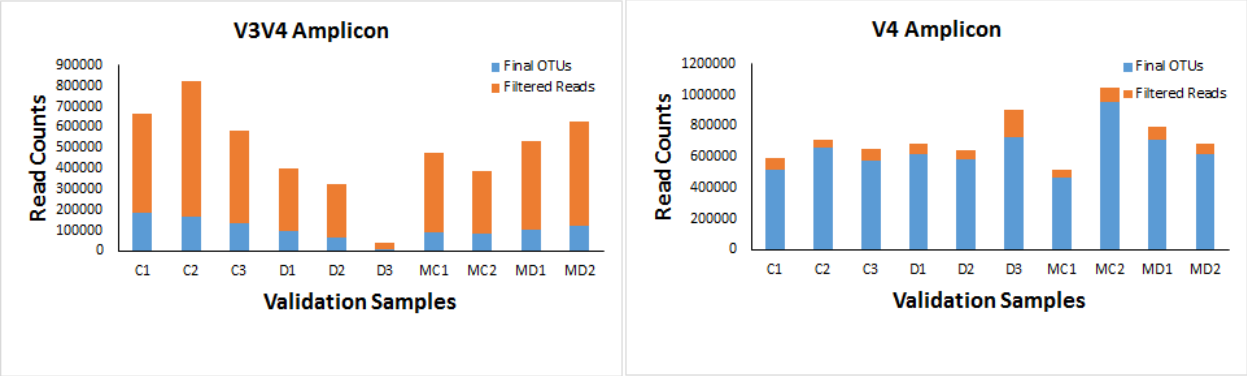

Figure 19. Amplicon V3V4 has higher failed reads compared to amplicon V4.

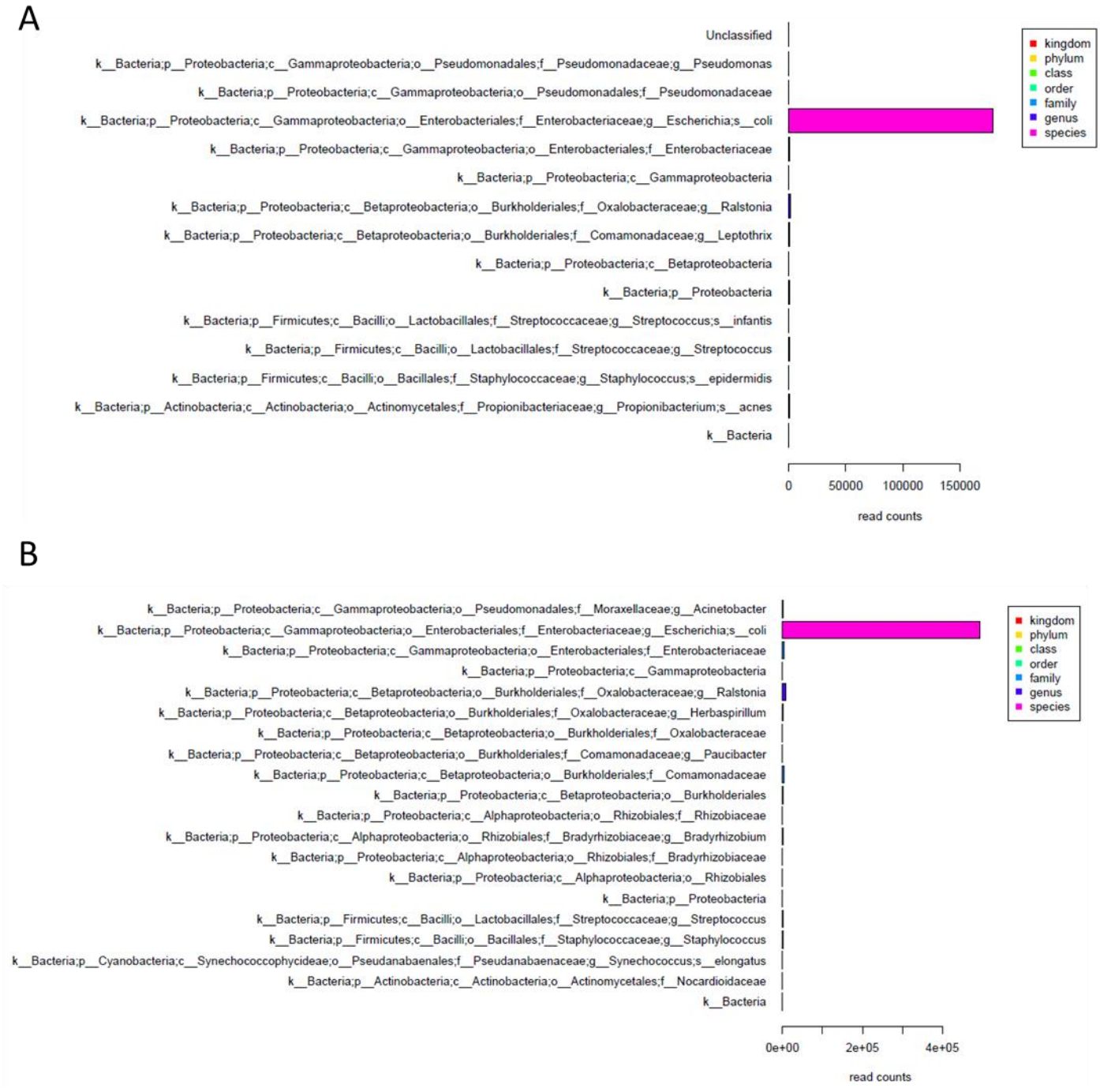

Figure 20. Customized data analysis from Illumina metagenomics workflow allows accurate species identification in C1 (Escherichia coli Culture) for both amplicons V3V4 (A) and V4 (B).

A Illumina Customized Analysis V3V4

Samples	Single Organism Culture			Culture Mix		Single Organism gDNA			gDNA Mix	
	C1	C2	C3	MC1	MC2	D1	D2	D3	MD1	MD2
Escherichia coli										
Staphylococcus epidermidis										
Cyanobacterium Synechococcus sp. IU 625										

B Illumina Customized Analysis V4

Samples	Single Organism Culture			Culture Mix		Single Organism gDNA			gDNA Mix	
	C1	C2	C3	MC1	MC2	D1	D2	D3	MD1	MD2
Escherichia coli										
Staphylococcus epidermidis										
Cyanobacterium Synechococcus sp. IU 625										

Family Genus Species

Figure 21. Identification in single and polymicrobial samples from customized Ion 16S metagenomics workflow for both amplicons V3-V4 (A) and V4 (B). Genus or species level was identified in all samples.

Validation on genomic DNA mixture of 20 bacterial strains on illumina 16S V4 workflow

To further investigate Illumina V4 metagenoics workflow, Genomic DNA from Microbial Mock Community B containing twenty different bacteria strains was analyzed. All the strains were classified at the genus or species level accurately (Figure 22). Illumina V4 metagenoics workflow with customized analysis provided a rapid and sensitive method for the identification of bacterial species in polymicrobial samples. Samples can be highly multiplexed to reduce time and cost.

Establishing the sensitivity of illumina 16S V4 workflow

One microliter of library DNA from culture lysates and genomic DNA was accessed with D1k ScreenTape. Figure 23 showed the library of *Escherichia coli*, *Proteus vulgaris, Staphylococcus epidermidis*, and *Bacillus cereus*. The culture lysates showed the same amplicon size with genomic DNA. With index and adaptor, the amplicon size was 380 bp as expected. With further dilution, the library concentration decreased. All the single- and poly-microbial samples showed same amplification pattern. The library can be prepared from the culture lysates directly without DNA isolation. The NTC showed less amplification than 6-cell samples.

The libraries were sequenced and the proportion of final OTUs for the taxonomic assignment compared to the original read counts was calculated for different dilutions of culture lysates and genomic DNA after the QC and filtering steps as previous described. The different dilutions of culture lysates with above 60 bacterial cells generated the similar or even higher proportion of final usable OTUs for taxonomic assignment with bacterial genomic DNA. With decrease of the cell number to about 6, the fraction of final OTUs decreased. The NTC showed less final usable OTUs compared to gDNA (Figure 24).

Taxonomy was assigned to all the samples based on the final OTUs. For the single-microbial samples, the genus or species taxonomy was accurately assigned to each isolated bacterial genomic DNA. The culture lysates with above 60 cells showed consistent taxonomic identification with genomic DNA. More than 99% of total reads were assigned to the correct genus or species level. For the culture lysates with about 6 cells, a dominant fraction of reads were assigned to correct genus or species level. None of the four bacterial strains were detected in the NTC sample (Figure 25A). For the poly-microbial samples, all the total reads were accurately assigned to genus or species level for the artificial genomic DNA mixture and for the mixed culture lysates with above 60 cells. The four dilutions of culture lysates with more than 600 cells showed consistent composition of the four bacterial strains, which suggested that this method had the potential to be used for quantitative analysis of microbial structure when there are more than 600 bacterial cells. For the mixed culture lysates with around 6 cells, a dominant fraction of reads were assigned to correct genus or species level (Figure 25B).

Figure 26 shows all the genera detected on the single- or poly-microbial samples and NTC. When there were around 6 cells in the cultures, the contamination started to appear. The common contamination for Molecular Biology Grade water and PCR reagents including *Acinetobacter*, *Cupriavidus*, *Mesorhizobium*, *Pseudomonas*, *Ralstonia*, *Streptococcus*, and *Xanthomonas* were detected in the NTC sample[64]. None of the four bacterial strains discussed earlier were detected in the NTC sample.

Organism	Mock Community
Acinetobacter baumannii	
Actinomyces odontolyticus	
Bacillus cereus	
Bacteroides vulgatus	
Clostridium beijerinckii	
Deinococcus radiodurans	
Enterococcus faecalis	
Escherichia coli	
Helicobacter pylori	
Lactobacillus gasseri	
Listeria monocytogenes	
Neisseria meningitidis	
Propionibacterium acnes	
Pseudomonas aeruginosa	
Rhodobacter sphaeroides	
Staphylococcus aureus	
Staphylococcus epidermidis	
Streptococcus agalactiae	
Streptococcus mutans	
Streptococcus pneumoniae	

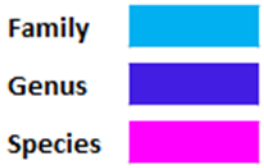

Figure 22. Taxonomic classification of microbial mock Community B containing twenty different bacteria strains. Illumina V4 metagenoics workflow with customized analysis was able to assign correct species or genus level identification in the mock polymicrobial sample.

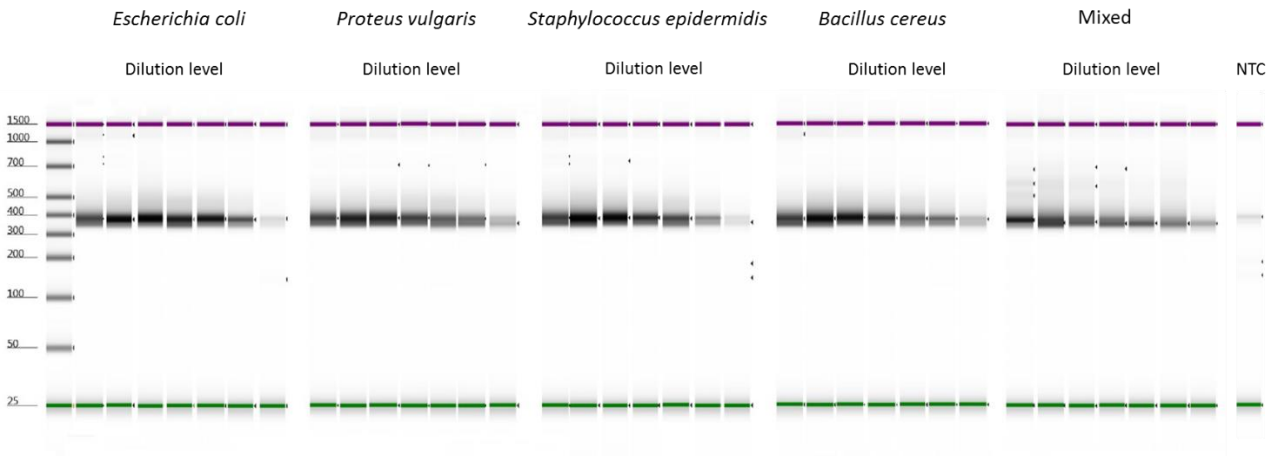

Figure 23. Library from cultures and DNA of single- or poly-microbial samples. With decrease of the cell number, the concentration of library decreased. The library size from the culture lysates was the same with genomic DNA.

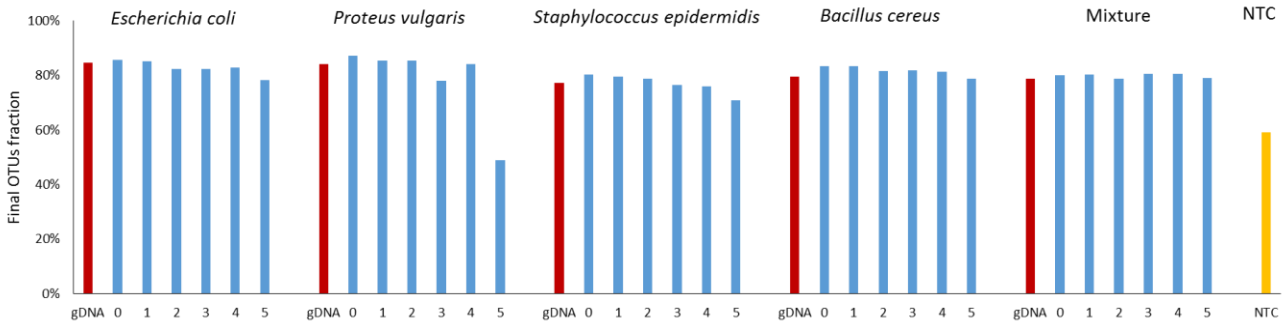

Figure 24. Proportion of final OTUs from cultures and DNA of single- or poly-microbial samples. The red bars represent the genomic DNA, the blue bars represent different dilution of cultures, and the yellow bar represents the negative control. The culture lysates with above 60 bacterial cells showed the similar proportion of final usable OTUs with bacterial genomic DNA. With decrease of the cell number to around 6, the fraction of OTUs for taxonomic assignment decreased.

A

Samples		Single-microbial Samples			
		Escherichia coli	*Proteus vulgaris*	*Staphylococcus epidermidis*	*Bacillus cereus*
gDNA		100%	100%	100%	100%
Culture lysates	0	100%	100%	100%	100%
	1	100%	100%	100%	100%
	2	100%	100%	100%	100%
	3	100%	100%	99%	100%
	4	100%	100%	100%	100%
	5	93%	96%	70%	100%
NTC		0%	0%	0%	0%

B

Samples		Poly-microbial Samples				Total Fraction
		Escherichia coli	*Proteus vulgaris*	*Staphylococcus epidermidis*	*Bacillus cereus*	
gDNA		41%	14%	12%	34%	100%
Culture lysates	0	36%	33%	8%	23%	100%
	1	32%	32%	10%	25%	100%
	2	39%	31%	8%	22%	100%
	3	40%	35%	6%	19%	100%
	4	48%	39%	4%	9%	100%
	5	64%	28%	0%	2%	94%

Genus Species

Figure 25. Taxonomic identification in single- (A) and poly-microbial (B) samples. Blue represents the genus level assignment and purple represents the species level assignment. In NTC sample, there is no detection of any of the four bacterial strains.

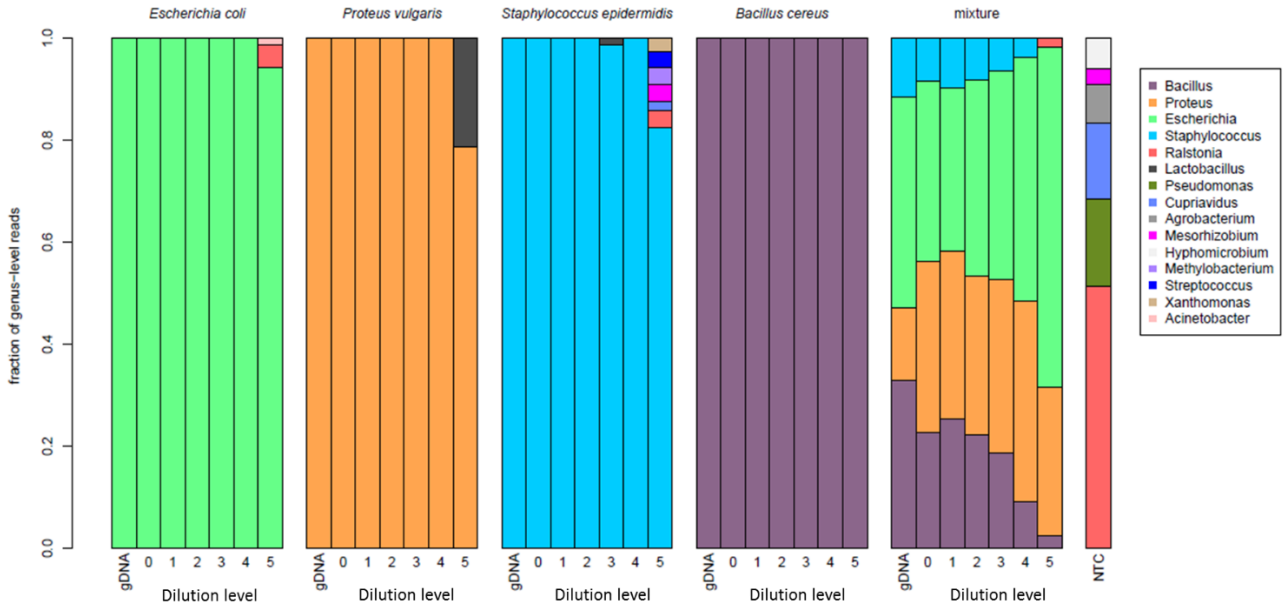

Figure 26. Abundance of genera from single- and poly-microbial samples and NTC.

Characterizing the microbiome at the time of embryo transfer

A total of 395 patients were included in the study. Genus-level taxonomy was assigned based on the final OTUs from the 395 patients. The data-set was then filtered to consider only those genus calls that were present in at least one sample at a relative abundance > 1%. There were a total of 248 different genus calls present across patient samples. Vaginal bacteria *Lactobacillus*, *Corynebacterium*, *Bifidobacterium*, *Staphylococcus* and *Streptococcus* were detected. These bacteria strains had been identified in other endometrium studies[65,66,67].

The fraction of read counts of each genus was charactrized at time of transfer for those patients with ongoing pregnancy vs. those without ongoing pregnancy. No differences between the two status groups were large enough to survive multiple test corrections. *Lactobacillus* was detected in all the samples. Figure 27 represented the fraction of read counts of *Lactobacillus*, which didn't differ between the two groups (p=0.464). To characterize the diversity of the samples, the Shannon diversity index (SDI) were utilized (Figure 28). There was no difference between the two groups (p=0.164).

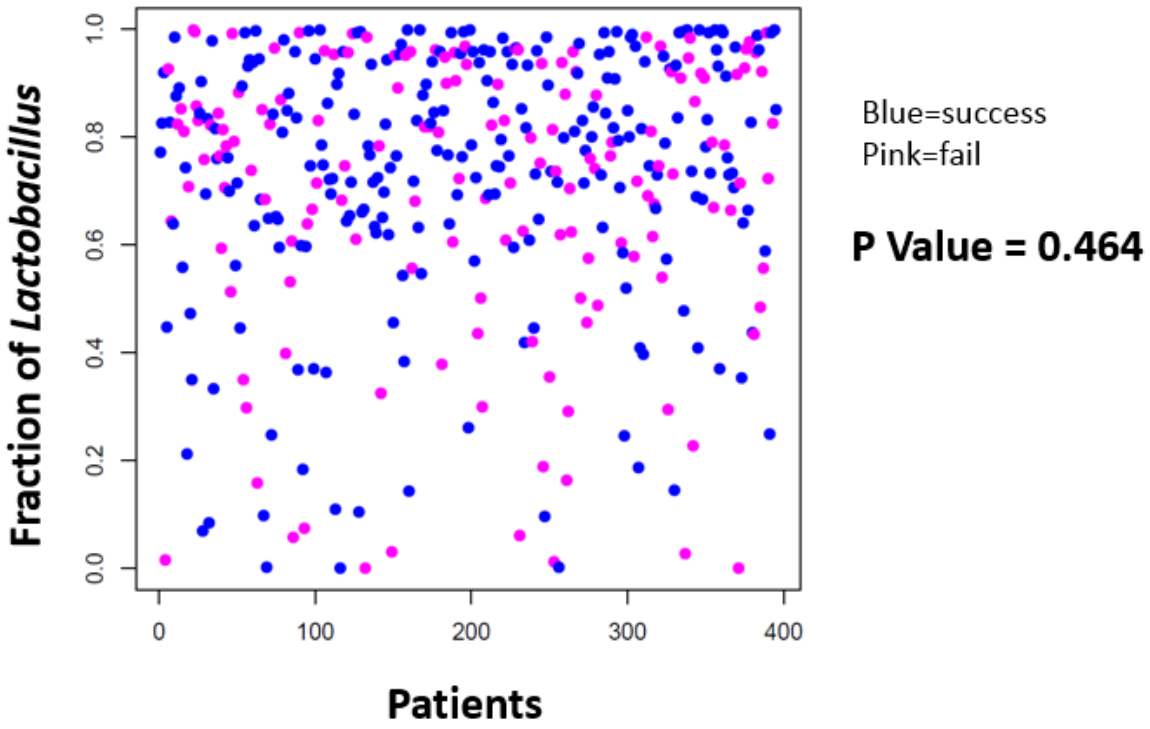

Figure 27. Fraction of *Lactobacillu*. *Lactobacillus* was detected in all 395 samples, but there is no difference between the two patient groups.

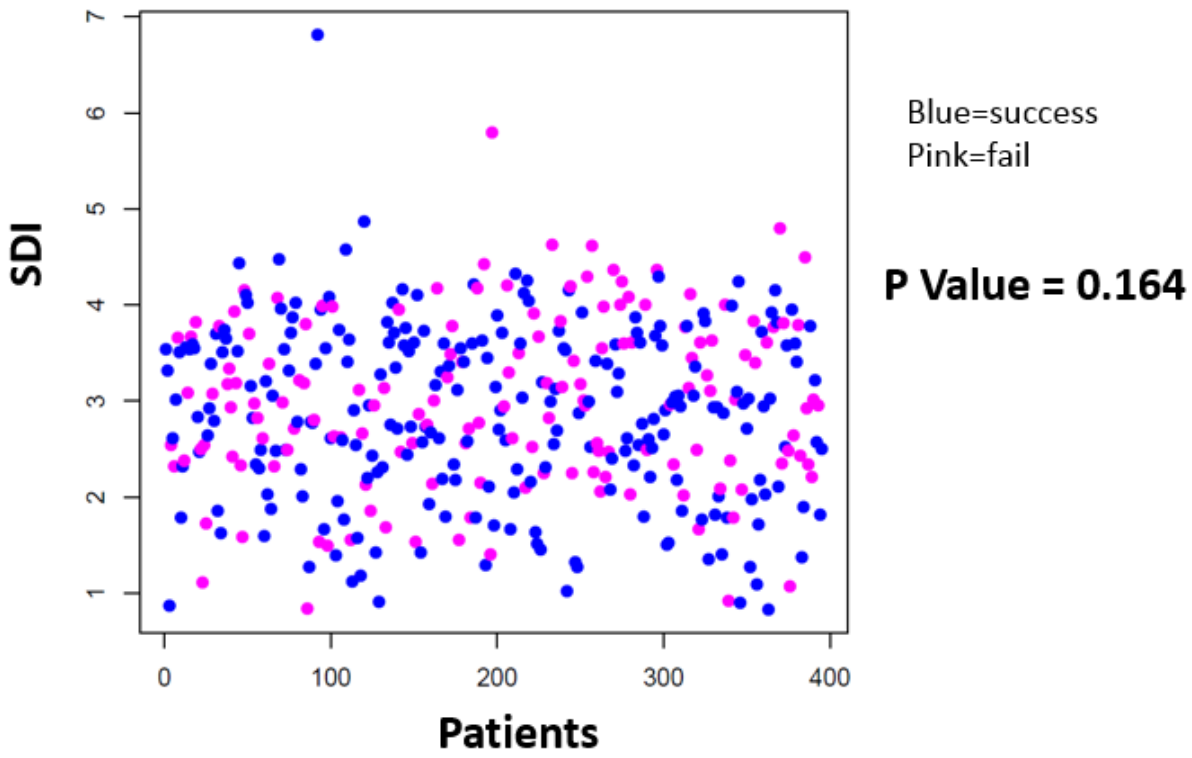

Figure 28. Shannon Diversity Index, which is a quantitative measure that reflects how many different species in a community. There was no difference between the two patient groups.

Discussion

Given the need to develop more robust markers for reproductive success and the fact that oocyte competence, both ploidy status and cytoplasmic competence, as well as the inflammatory and immune environment at the time of embryo implantation have been identified as major barriers to reproductive success, our goal was to address key markers involved in each of these processes.

Mouse aneuploidy model and Reproduction

In these studies we validated a sophisticated comprehensive chromosome screening method using single cell controls from MEFs of known trisomy, then applied this method in mouse gametes (oocytes and polar bodies) and preimplantation embryos. Using WGA, DNA from single gametes (polar bodies and oocytes) and blastocysts was reliably amplified, and comprehensive and quantitative analysis of the ploidy status was performed using NGS. The lack of the Y chromosome in oocytes, and the identification of reciprocal aneuploidies in matched oocyte and polar body pairs further validated our WGA and NGS based CCS.

We observed that aneuploid rate from mice of advanced reproductive age was from 1-20% per female in our study, which is lower that what has been reported previously[12,68,69,70]. It was reported that the incidence of aneuploidy to be 50% in B6D2F1 mice of advanced reproductive age[12], and 37.5% in CD1 mice at 12 months[20]. There are several explanations for this apparent discrepancy. The sequencing method we used may not distinguish sister chromatids that have prematurely separated at metaphase II that would mis-segregate and contribute to aneuploidy upon completion of meiosis II following fertilization. This could result in an underestimation of the aneuploidy incidence because premature dyad separation in meiosis II may be a major origin of segregation error in mouse oocytes. To fully elucidate these mechanisms, future studies

performing CCS in the oocyte, first and second polar bodies are warranted to distinguish reproductive age-associated aneuploidies specifically due to meiosis I and II errors.

It was also found that the frequency of aneuploidy observed in IVM blastocysts (30.8%) from aged mice was markedly higher than in the IVM oocytes (15%) in our study. This may be due to a number of factors including the additional contribution of meiosis II and post-zygotic mitotic errors, the use of ovarian stimulation to obtain eggs for blastocyst production, the potential strain-specific differences in susceptibility to age related aneuploidy, and the difference in media and protocols used for obtaining oocytes and embryos. All of these factors represent areas of great interest for future investigation using this technology and model system.

With this technology, we were able to obtain quantitative copy number information, providing insight into the type of meiotic errors that occur – either nondisjunction of homologous chromosomes (a copy number of four or zero for a particular chromosome in the respective matched oocyte and polar body samples) or premature separation of sister chromatids (PSSC) (a copy number of three or one for a particular chromosome in the respective matched oocyte and polar body samples). We identified 6 aneuploid oocytes in this study, and the aneuploidy was attributed to PSSC in 5 of the oocytes. Only one was due to nondisjunction of homologous chromosomes. These findings are consistent with previous mouse studies and clinical data from human ART in which most aneuploidies are due to PSSC rather than nondisjunction[71,72]. In fact, age-associated loss of centromeric cohesion has been identified as a prime mechanism underlying PSSC in the mouse and human[18,73]. Our findings, therefore, add to the evidence that the aging mouse may provide a relevant model for the mechanisms of aneuploidy development in the human oocyte.

When analyzing blastocysts, CCS using WGA and NGS confirmed the lower incidence of aneuploidy in blastocysts originating from young females compared to aged females, which is consistent with previous mouse and human studies [7,8,10,11,12]. Whereas there was no difference in aneuploidy in young females associated with the type of oocyte maturation used, blastocysts from females of advanced maternal age produced after IVM had more aneuploid embryos compared to IVO blastocysts, suggesting a susceptibility of older females to chromosome errors after IVM. In IVO, the oocyte maturation process involves a number of signaling pathways and depends on the close interaction between the cumulus cells and the oocyte[74]. It has been reported that mouse oocytes produced via IVO had higher fertilization and blastocyst formation rates than IVM[75,76]. It was also found that oocytes have a higher frequency of abnormal meiotic spindles and chromosomal mis-alignment after IVM[77]. This finding implies that oocyte maturation method play an important role in the oogenesis and embryogenesis, especially in the older mice.

Taken together, our results demonstrate that CCS using WGA and NGS is a robust technique to evaluate chromosome segregation errors that can be applied to gametes and embryos of any species with a published and annotated genome. Moreover, this method is highly cost-effective making it accessible for use in most laboratories[78]. Because this technology identifies aneuploidy in a chromosome-specific and quantitative manner, this approach provides the field of reproductive science and medicine with a new tool for evaluating how age, environmental factors, and disease conditions influence aneuploidy in the gamete and preimplantation embryo. In addition, it could be used in future research to assess the effectiveness of therapeutic interventions to lower the incidence of oocyte and embryo aneuploidy in aged females.

Competence Mitochondria in Reproductive Competence

The mouse model has been widely used as a model system to gain insight into the key aspects of human reproductive biology. Recently, we were the first to establish a WGA and NGS based CCS method to further inform our fundamental understanding of aneuploidy in mouse oocytes and preimplantation embryos. Here we extended these studies by validating a method for simultaneous quantification of mtDNA content from limited amounts of starting material. Cultured mouse cells were treated with EtBr to generate cells with reduced levels of mtDNA. Single-cell samples were collected to mimic a polar body or oocyte, and 100-cell samples were collected to represent a blastocyst. The WGA and NGS based method detected the decrease in mtDNA content with longer exposure to EtBr in both samples. Single cells showed higher variation than 100-cell samples, which may be due to cell cycle asynchrony or differences between individual cells in how they were affected by EtBr treatment.

In addition to *in vitro* validation, our detection of a much higher level of mtDNA in oocytes as compared to polar bodies is consistent with the expectation that highly asymmetric division of the cytoplasm in meiosis results in accumulation of mtDNA in the oocyte for later embryo development [79]. The assay was further validated by the comparison of mtDNA content in oocytes and blastocysts. Most publications suggested that there is no mtDNA replication until implantation, so each newly divided blastomere within the pre-implantation embryo will possess fewer copies of the mtDNA at each stage of post-fertilization cell division[80,81,82]. In our study, the average mtDNA content in oocytes was 180- fold higher than the cells in blastocysts, indicating that there are about 7 to 8 rounds of cell division from fertilized oocytes to blastocysts. This finding is consistent with mouse embryonic development, in which a zygote undergoes 8 to 10 cell divisions to form a morula and then further develops into a blastocyst.

In this study, we found that relative mtDNA content was associated with ploidy status, maternal age, and oocyte maturation methods in mouse blastocysts. The difference of relative mtDNA level between the groups was significant with the implementation of the correction factor based on the gender and ploidy.

Relative mtDNA content in aneuploid mouse embryos was found to be significantly higher than euploid embryos, which is consistent with observations in humans[6,7]. Increased mtDNA copy number was observed in aneuploid oocytes from diabetic mice[83]. Mitochondrial biogenesis and adequate energy production are important for cytoplasmic maturation, embryogenesis and placentation[84],[85]. There is a hypothesis that the mtDNA copy number in the embryo is not a direct indicator of energetic capability but rather is an indicator of energetic stress[10]. The observation of increased mtDNA content in aneuploid embryos in our study suggests that aneuploid embryos may need more energy for chromosome segregation, and activate mitochondrial biogenesis at an earlier stage of embryo development.

Mouse maternal age was associated with the relative mtDNA content of embryos; relaitive mtDNA content in mouse embryos increased with maternal age. Previous studies showed that reproductively old humans and animals tend to have lower mtDNA copy numbers or more dysfunctional mitochondria in their oocytes[86,87,88]. One explanation for the age related mtDNA increase in the embryos is that a reduced number of mitochondria may produce an inadequate energy supply for embryonic development and therefore trigger early mitochondrial biogenesis and increased mitochondrial number in preimplantation embryos. Similar results were observed in human embryos[7,89]. Another explanation is related to mitophagy, which is the selective degradation of mitochondria by autophagy and occurs to defective mitochondria following damage or stress. It promotes turnover of mitochondria and prevents accumulation of

dysfunctional mitochondria[90]. It was found that mitophagy may play a key role in retarding accumulation of somatic mutations of mtDNA with aging[91]. In the process of embryogenesis, mitophagy might be impaired in the embryos from old mice, which causes the accumulation of dysfunctional mitochondria, and therefore higher level of mtDNA is observed.

It has been reported that mouse oocytes produced via IVO had higher fertilization and blastocyst formation rates than IVM[92,93]. Embryos derived via IVO also had a lower anueploidy rate[11]. Those findings imply that oocyte maturation method play an important role in the oogenesis and embryogenesis. In our study, we quantified the relative mtDNA level related to cytoplasmic maturation, and we found relative mtDNA content was higher in embryos derived from IVO compared to IVM. Oocytes derived from IVO have higher quality compared to IVM, so they may accumulate higher quantity of mtDNA during oogenesis, which could facilitate fertilization and embryo development[94]. Lower level of mtDNA in embryos derived from IVM, due to inadequate mitochondrial biogenesis or cytoplasmic maturation, may adversely affect oocyte quality, so age and IVM may have different mechanisms that underlie oocyte quality.

In conclusion, the mouse study provides a validated method to assess the relative mtDNA content in mouse oocytes, polar bodies and blastocysts that can be performed simultaneously and in conjunction with CCS. The method could be applied in future research to assess the effectiveness of therapeutic interventions involving mitochondrial copy number and distribution. Although this study suggests that mtDNA copy number alone can be associated with embryonic reproductive competence, future work is needed to understand the relationship between mtDNA quantity and implantation success after embryo transfer in mice. Studies of mitochondrial number and function in mouse oocytes and embryos may help to elucidate basic mechanisms of mitochondrial biogenesis and function related to reproductive competence.

Prior human studies observed a relationship between mtDNA content and outcomes, it is unclear whether this relationship only identified poor prognosis patients from good prognosis patients. In other words, mtDNA content may have been a surrogate for age and not an additional variable that improves selection. In our human embryo study, a stepwise approach was used to preform accurate mtDNA quantification on embryo biopsy material. Paired comparisons of mitochondrial DNA content were performed on euploid sibling embryos as opposed to comparing embryos belonging to different parents. This methodology eliminates patient-specific variables leading to a well-controlled investigation of the predictive value of mtDNA for reproductive outcome in a single cohort.

This study investigated the relationships between mtDNA quantity and multiple clinical parameters available during IVF cycles. A significant association was found between mitochondrial quantity and maternal age providing evidence that preimplantation blastocysts developed from older patients have lower levels of mtDNA compared with those from younger ones. The association of age and mtDNA content has been studied previously in both oocytes and embryos. Studies evaluating oocyte mitochondrial levels appear to be in agreement with the present study, showing decreasing levels in older patients[21]. However, the opposite effect was recently shown in a study evaluating blastocyst levels, explaining that perhaps blastocysts from older women have more demanding energy requirements due to a continuously declining organelle function over time[95] [10]. Additionally, a comparison of embryos biopsied on Day 5 versus Day 6 identified that mitochondrial content per cell may decline during blastocyst development. Evaluation of blastocyst morphology also revealed significant associations. Embryos identified to have superior morphologic qualities were found to contain lower quantities of mtDNA. These associations may reflect that mitochondrial DNA content is

impacted by the degree of expansion and mitogenic activity of the blastocyst. For example, blastocysts that have experienced more cell divisions may be expected to have different levels mitochondrial DNA than those that have not based on partitioning of available mitochondria.

Of particular clinical importance is the potential use of mtDNA quantity as a modality to predict embryo success. Proper evaluation of a marker for its ability to predict outcomes among sibling embryos is challenging, but it can be accomplished using a variety of study designs that allow for control over known and unknown patient-specific variables. By analyzing only those patients undergoing DET's and identifying the implanted embryo, the predictive values of a marker for reproductive potential can be truly isolated. Identification can be achieved using gender if sibling embryos are of different sex. Alternatively, fingerprinting analysis on the delivered offspring can be utilized regardless of gender. This approach is more complicated and costly, but the technology has been available and used in prior studies successfully[96,97,98]. This is the largest study to date evaluating the predictive value of mtDNA content using a sibling embryo study design. We identified 69 cases where both a euploid male and female embryo were transferred simultaneously and resulted in a singleton outcome. A paired analysis revealed that mtDNA levels were not predictive of a successful outcome. Based on these results, the current available data suggests that mtDNA quantification is insufficient in its ability to enhance embryo selection over current, more validated techniques.

Endometrial Microbiome and Reproductive Competence

The population of microbes in and on the human body has become better characterized as a result of the National Institute of Health's Human Microbiome Project. The vaginal microbiome at the lower part of female reproductive tract has been widely studied; however, the uterine microbiome in general and, in particular, at the time of embryo transfer in the peri-implantation period is largely

uncharacterized. Recent studies of the uterine endometrial microbiome[99] suggest that further characterization of this microbial environment could be vital in understanding endometrial proliferation; embryo apposition, attachment, and invasion; and the development of early pregnancies.

Given that during IVF embryos are placed into the uterine cavity utilizing a transfer catheter, this represents an ideal time to obtain biological material for microbiome analysis without altering clinical care provided the catheter tip can be analyzed requiring no further sampling. This technique involves no additional trauma to the endometrial cavity which might impact clinical outcomes and does not require endometrial tissue sample processing in the laboratory. However, the major challenge presented in this approach, as is often the case when approaching diagnostics in the pre- and peri-implantation period, is that the amount of bacteria in the catheter tips and the starting DNA material may be very little and thus difficult to be analyzed. In this study, we developed the 16S rRNA based NGS to characterize endometrial microbial environment by analyzing the transfer catheter tips.

A small amount of bacterial culture (~1000 bacteria) was lysed and followed by amplification directly to validate the classification of the bacteria. Both Ion and Illumina 16S metagenomics workflows were tested in our study. The analyses from Ion reporter detected only the family level for the validation samples, and the built-in analyses from Illumina MiSeq didn't assign the correct genus or species calls for all the validation samples. Customized analyses were carried out which was able to improve the taxonomic assignment. Although the genus and species level assignment were improved with the custom analysis when comparted to the Ion 16S Metagenomics workflow, the majority of the reads were still only able to be characterized at the family level. Another issue

with the Ion 16S workflow was the bias amplification of the seven hypervariable regions, which caused issues with quantitative analysis of the microbiome.

For Illumina 16S Metagenomics workflow, our customized analyses identified genus or species for all the samples for both V3-V4 and V4 amplicons. Amplicon V4 had higher final usable reads compared to amplicon V3-V4 for all the samples, which was due to the fact that V3-V4 is longer than V4. The error frequency of the sequencing is increased for longer reactions, and joining the longer sequence is more difficult because the overlap sequences for read 1 and read 2 are shorter. To further validate the taxonomic identification of V4 amplicon, genomic DNA mixture of 20 bacterial strains was tested and all the species or genus were detected. Further, the Illumina 16S rRNA V4 metagenomics workflow allowed higher number of multiplexed samples for one sequencing run to reduce time and cost with reliable genus and species classification.

To validate the direct lysis procedure based on Illumina V4 workflow, two Gram-negative bacteria (*Escherichia coli* and *Proteus vulgaris*) and two Gram-positive bacteria (*Staphylococcus epidermidis*, and *Bacillus cereus*) were tested on lysates from different culture dilution and isolated genomic DNA. Artificial mixtures of bacterial culture and DNA were tested to prove that taxonomy can be assigned to poly-microbial samples, which represented the real human microbial community. For both Gram-positive and negative bacteria, despite cell wall structural differences, the genus and/or species taxonomic level was accurately detected for both single- and poly-microbial samples when there were more than 60 bacterial cells in the culture lysates. This method can reliably detect the taxonomy from the cell lysates with more than 60 bacterial cells directly. One bacterial cell has 1.5 to 4 fg DNA, therefore 60 cells have about 90 to 240 fg DNA. The current Illumina 16S metagenomic workflow requires 12.5 ng DNA to start with,

which requires a large amount of bacterial cells. Our method provided a sensitive approach to study the ultra-low amount of bacteria from the environment.

Recent studies of the uterine endometrial microbiome suggest that further characterization of this microbial environment could be vital in understanding endometrial proliferation; embryo apposition, attachment, and invasion; and the development of early pregnancies[100]. Given that during IVF embryos are placed into the uterine cavity utilizing a transfer catheter, this represents an ideal time to obtain biological material without altering clinical care provided, and the catheter tip can be analyzed requiring no further sampling. This technique involves no additional trauma to the endometrial cavity which might impact clinical outcomes and does not require endometrial tissue sample processing in the laboratory. However, the major challenge presented in this approach, as is often the case when approaching diagnostics in the pre- and peri-implantation period, is that the amount of bacteria in the catheter tips may be very low and thus difficult to be analyzed. The lysis direct technique overcame the challenge and characterized endometrial microbial environment by analyzing the transfer catheter tips.

A total of 395 embryo transfer catheter tips were analyzed in this study. Vaginal bacteria *Lactobacillus, Corynebacterium, Bifidobacterium, Staphylococcus* and *Streptococcus* were detected in the uterus endometrium. *Lactobacillus* abundance was detected in all the samples as might be expected. *Lactobacillus* species have major functions in the reproductive tract including pH maintenance, prevention of long-term colonization of the harmful bacteria by adhering to reproductive tract epithelial cells, and production of lactic acid, hydrogen peroxide and bacteriocins. This allows for competitive inhibition of other pathologic bacteria in the reproductive tract.

The data in this study showed the microbiome at the time of ET may differ by pregnancy outcome but highlighted the challenge of low bacterial load and read counts when analyzing ET catheter tips alone. In order to more fully investigate the microbiome's affect utilizing this robust analytic technique, specimens with a more reliable and higher bacterial load would be required. Better characterization of the microbiome at the time of embryo transfer may yield microbiome profiles which are favorable and unfavorable when it comes to reproductive outcomes. Once this is established, intervening, either with antibiotics or probiotics, would be a natural clinical application to see if the microbiome profile could alter the reproductive outcomes.

Literature Cited

[1] Chandra A., Copen CE, Stephen EH. Infertility and Impaired Fecundity in the United States, 1982–2010: Data From the National Survey of Family Growth. National Health Statistics Reports, Number 67, Aug 14th, 2013.

[2] Faddy MJ, Gosden RG, Gougeon A, Richardson SJ, Nelson JF. Accelerated disappearance of ovarian follicles in mid-life: implications for forecasting menopause. Hum Reprod 1992;7:1342–6.

[3] Broekmans FJ, Kwee J, Hendriks DJ, Mol BW, Lambalk CB. A systematic review of tests predicting ovarian reserve and IVF outcome. Hum Reprod Update 2006;12:685–718.

[4] Simpson JL. Genetic programming in ovarian development and oogenesis. In: Lobo RA, Kelsey J, Marcus R, editors. Menopause: biology and pathology. San Diego (CA): Academic Press; 2000:77–94.

[5] Eppig JJ. Coordination of nuclear and cytoplasmic oocyte maturation in eutherian mammals. Reprod Fertil Dev 1996; 8:485-489.

[6] Hyman RW, CN, Jiang H, Palm C, Fukushima M, Bernstein D, Vo KC, Zelenko Z, Davis RW,and Giudice LC. The dynamics of the vaginal microbiome during infertility therapy with in vitro fertilization-embryo transfer. J Assist Reprod Genet. 2012; 29(2):105–115.

[7] Krisher RL. The effect of oocyte quality on development. J Anim Sci. 2004;82(E-Suppl):E14–23.

[8] Eppig JJ. Coordination of nuclear and cytoplasmic oocyte maturation in eutherian mammals. Reprod Fertil Dev 1996; 8:485-489

[9] Hunt PA, Hassold TJ. Human female meiosis: what makes a good egg go bad? Trends Genet 2008; 24:86-93.

[10] Hassold T, Hunt P. Maternal age and chromosomally abnormal pregnancies: what we know and what we wish we knew. Curr Opin Pediatr. 2009;21:703–8.

[11] Munne S, Alikani M, Tomkin G, Grifo J, Cohen J. Embryo morphology, developmental rates, and maternal age are correlated with chromosome abnormalities. Fertil Steril. 1995;64:382–91.

[12] Gosden R, Lee B. Portrait of an oocyte: our obscure origin. J Clin Invest 2010; 120:973-983.

[13] Franasiak JM, Forman EJ, Hong KH, Werner MD, Upham KM, Treff NR, Scott RT, Jr. The nature of aneuploidy with increasing age of the female partner: a review of 15,169 consecutive trophectoderm biopsies evaluated with comprehensive chromosomal screening. Fertil Steril 2014;101:656-663

[14] Balasch J, Gratacos E. Delayed childbearing: effects on fertility and the outcome of pregnancy. Curr Opin Obstet Gynecol 2012;24:187–93.

[15] Gossett DR, Nayak S, Bhatt S, and Bailey SC. What Do Healthy Women Know About the Consequences of Delayed Childbearing? J Health Commun. 2013;18:118–128.

[16] Merriman JA, Jennings PC, McLaughlin EA and Jones KT. Effect of aging on superovulation efficiency, aneuploidy rates, and sisterchromatid cohesion in mice aged up to 15 months. Biol. Reprod. 2012;86:49

[17] Kuliev A, Zlatopolsky Z, Kirillova I, Spivakova J and Cieslak JJ. Meiosis errors in over 20,000 oocytes studied in the practice of preimplantation aneuploidy testing. Reprod. Biomed. Online. 2011; 22, 2-8.

[18] Pan H, Ma P, Zhu W, Schultz RM. Age-associated increase in aneuploidy and changes in gene expression in mouse eggs. Dev Biol 2008; 316:397-407.

[19] Scott RT, Upham KM, Forman EJ, Hong KH, Scott KL, Taylor D, Tao X, Treff, NR. Blastocyst biopsy with comprehensive chromosome screening and fresh embryo transfer significantly increases in vitro fertilization implantation and delivery rates: a randomized controlled trial. Fertil Steril. 2013;100:697-703.

[20] Werner MD, Scott RT Jr, Treff NR. 24-chromosome PCR for aneuploidy screening. Curr Opin Obstet Gynecol. 2015;27:201-5.

[21] Handyside AH. 24-chromosome copy number analysis: a comparison of available technologies. Fertil Steril 2013;100:595-602.

[22] Scott RT, Upham KM, Forman EJ, Hong KH, Scott KL, Taylor D, Tao X, Treff, NR. Blastocyst biopsy with comprehensive chromosome screening and fresh embryo transfer significantly increases in vitro fertilization implantation and delivery rates: a randomized controlled trial. Fertil Steril. 2013;100:697-703.

[23] Hunt PA, Hassold TJ. Human female meiosis: what makes a good egg go bad? Trends Genet. 2008;24:86-93.

[24] Voet D, Voet JG, Pratt CW. Fundamentals of Biochemistry, 2nd Edition. John Wiley and Sons, Inc. 2006

[25]Murphy, MP. How mitochondria produce reactive oxygen species. Biochem J. 2009;417:1-13

[26] Huang K, Manton KG. The role of oxidative damage in mitochondria during aging: A review. Front Biosci. 2004;9:1100-17.

[27] Wiesner RJ, Rüegg JC, Morano I. Counting target molecules by exponential polymerase chain reaction: copy number of mitochondrial DNA in rat tissues. Biochem Biophys Res Commun. 1992;183:553-9.

[28] Su J, Tao X, Baglione G, Treff NR, Scott RT. Mitochondrial DNA is significantly increased in aneuploid human embryos. Fertil Steril. 2010;94:S88-9.

[29] Fragouli E, Spath K, Alfarawati S, Kaper F, Craig A, Michel CE et al. Altered levels of mitochondrial DNA are associated with female age, aneuploidy, and provide an independent measure of embryonic implantation potential. PLoS genetics. 2015;11:e1005241.

[30] Stigliani S, Persico L, Lagazio C, Anserini P, Venturini PL, Scaruffi P. Mitochondrial DNA in Day 3 embryo culture medium is a novel, non-invasive biomarker of blastocyst potential and implantation outcome. Mol Hum Reprod. 2014;20:1238-46.

[31] Diez-Juan A, Rubio C, Marin C, Martinez S, Al-Asmar N, Riboldi M, Díaz-Gimeno P, Valbuena D, Simón C. Mitochondrial DNA content as a viability score in human euploid embryos: less is better. Fertil Steril. 2015;104:534-41.

[32] Treff NR, Krisher RL, Tao X, Garnsey H, Bohrer C, Silva E, Landis J, Taylor D, Scott RT, Woodruff TK, Duncan FE. Next Generation Sequencing-Based Comprehensive Chromosome Screening in Mouse Polar Bodies, Oocytes, and Embryos. Biol Reprod. 2016;94:76.

[33] Jones,KT, Lane,SI. Molecular causes of aneuploidy in mammalian eggs. Development. 2013;140:3719-30

[34] Merriman JA, Jennings PC, McLaughlin EA and Jones KT. Effect of aging on superovulation efficiency, aneuploidy rates, and sisterchromatid cohesion in mice aged up to 15 months. Biol Reprod. 2012;86:49.

[35] Kuliev A, Zlatopolsky Z, Kirillova I, Spivakova J and Cieslak JJ. Meiosis errors in over 20,000 oocytes studied in the practice of preimplantation aneuploidy testing. Reprod Biomed. 2011;22:2-8.

[36] MacLennan M, Crichton JH, Playfoot CJ, Adams IR. Oocyte development, meiosis and aneuploidy. Semin Cell Dev Biol. 2015;45:68-76.

[37] Eppig JJ. Coordination of nuclear and cytoplasmic oocyte maturation in eutherian mammals. Reprod Fertil Dev. 1996;8:485-489.

[38] Downs SM. Regulation of the G2/M transition in rodent oocytes. Mol Reprod Dev. 2010;77:566–85.

[39] Cotterill M, Harris SE, Collado Fernandez E, Lu J, Huntriss JD, Campbell BK, Picton HM. The activity and copy number of mitochondrial DNA in ovine oocytes throughout oogenesis in vivo and during oocyte maturation in vitro. Mol Hum Reprod. 2013;19:444-50.

[40] Nacarelli T, Azar A, Sell C. Inhibition of mTOR Prevents ROS Production Initiated by Ethidium Bromide-Induced Mitochondrial DNA Depletion. Front Endocrinol. 2014;5:122

[41] Victor AR, Brake AJ, Tyndall JC, Griffin DK, Zouves CG, Barnes FL, Viotti M. Accurate quantitation of mitochondrial DNA reveals uniform levels in human blastocysts irrespective of ploidy, age, or implantation potential. Fertil Steril. 2017;107:34-42.

[42] Diez-Juan A, Rubio C, Marin C, Martinez S, Al-Asmar N, Riboldi M, Díaz-Gimeno P, Valbuena D, Simón C. Mitochondrial DNA content as a viability score in human euploid embryos: less is better Fertil Steril. 2015 Sep;104(3):534-541.

[43] Scott RT 3rd, Su J, Tao X, Forman EJ, Hong KH, Taylor D, Treff NR. Trophectoderm DNA fingerprinting by quantitative real-time PCR successfully distinguishes sibling human embryos. J Assist Reprod Genet. 2014 Nov;31(11):1421-5.

[44] Treff NR, Tao X, Su J, Lonczak A, Northrop LE, Ruiz AA, Scott RT Jr. Tracking embryo implantation using cell-free fetal DNA enriched from maternal circulation at 9 weeks gestation. Mol Hum Reprod. 2011 Jul;17(7):434-8.

[45] Peterson J, Garges S, Giovanni M, McInnes P, Wang L, Schloss JA, et al. The NIH Human Microbiome Project. Genome Res 2009;19(12):2317–23.

[46] Blaser MJ and Plottel CS. Microbiome and malignancy. Cell Host & Microbiome. 2011; 10(4), 324-335.

[47] Davies J. In a map for human life, count the microbes, too. Science 2001;291(5512):2316.

[48] Relman DA, Falkow S. The meaning and impact of the human genome sequence for microbiology. Trends Microbiol 2001;9(5):206–8.

[49] Hyman RW, CN, Jiang H, Palm C, Fukushima M, Bernstein D, Vo KC, Zelenko Z, Davis RW,and Giudice LC. The dynamics of the vaginal microbiome during infertility therapy with in vitro fertilization-embryo transfer. J Assist Reprod Genet. 2012 Feb; 29(2): 105–115.

[50] Funkhouser LJ, Bordenstein SR. Mom knows best: the universality of maternal microbial transmission. PLoS Biol. 2013;11(8):e1001631.

[51] Schloss PD, Handelsman J. Status of the microbial census. Microbiol Mol Biol Rev. 2004;68:686–691.

[52] Kuczynski J, Lauber CL, Walters WA, Parfrey LW, Clemente JC, Gevers D, Knight R. Experimental and analytical tools for studying the human microbiome. Nature Reviews Genetics 2011;13 (1):47–58

[53] Caporaso JG, Lauber CL, Walters WA, Berg-Lyons D, Huntley J, Fierer N, Owens SM, Betley J, Fraser L, Bauer M, Gormley N, Gilbert JA, Smith G, Knight R. Ultra-high-throughput microbial community analysis on the Illumina HiSeq and MiSeq platforms. ISME J. 2012;6:1621–1624.

[54] Kozich JJ, Westcott SL, Baxter NT, Highlander SK, Schloss PD. Development of a dual-index sequencing strategy and curation pipeline for analyzing amplicon sequence data on the MiSeq Illumina sequencing platform. Appl Environ Microbiol. 2013;79:5112–5120.

[55] Shi W, Qin M, Chen F, Xia B. Supragingival Microbial Profiles of Permanent and Deciduous Teeth in Children with Mixed Dentition. PLoS One. 2016 Jan 11;11(1):e0146938.

[56] Munyaka PM, Eissa N, Bernstein CN, Khafipour E, Ghia JE. Antepartum Antibiotic Treatment Increases Offspring Susceptibility to Experimental Colitis: A Role of the Gut Microbiota. PLoS One. 2015 Nov 25;10(11):e0142536.

[57] Kasai C, Sugimoto K, Moritani I, Tanaka J, Oya Y, Inoue H, Tameda M, Shiraki K, Ito M, Takei Y, Takase K. Comparison of human gut microbiota in control subjects and patients with colorectal carcinoma in adenoma: Terminal restriction fragment length polymorphism and next-generation sequencing analyses. Oncol Rep. 2016 Jan;35(1):325-33.

[58] Al-Hebshi NN, Nasher AT, Idris AM, Chen T. Robust species taxonomy assignment algorithm for 16S rRNA NGS reads: application to oral carcinoma samples. J Oral Microbiol. 2015 Sep 29;7:289-34.

[59] Lagier JC, Armougom F, Million M, Hugon P, Pagnier I, Robert C, Bittar F, Fournous G, Gimenez G, Maraninchi M, Trape JF, Koonin EV, La Scola B, Raoult D. Microbial culturomics: paradigm shift in the human gut microbiome study. Clin Microbiol Infect. 2012 Dec;18(12):1185-93.

[60] Pfleiderer A, Lagier JC, Armougom F, Robert C, Vialettes B, Raoult D. Culturomics identified 11 new bacterial species from a single anorexia nervosa stool sample. Eur J Clin Microbiol Infect Dis. 2013 Nov;32(11):1471-81.

[61] Tang YC, Williams BR, Siegel JJ, Amon A. Identification of aneuploidy-selective antiproliferation compounds. Cell 2011; 144:499-512.

[62] Treff NR, Su J, Tao X, Levy B, Scott RT, Jr. Accurate single cell 24 chromosome aneuploidy screening using whole genome amplification and single nucleotide polymorphism microarrays. Fertil Steril 2010; 94:2017-2021

[63] Treff NR, Su J, Tao X, Levy B, Scott RT, Jr. Accurate single cell 24 chromosome aneuploidy screening using whole genome amplification and single nucleotide polymorphism microarrays. Fertil Steril 2010;94:2017-21.

[64] Salter SJ, Cox MJ, Turek EM, Calus ST, Cookson WO, Moffatt MF, Turner P, Parkhill J, Loman NJ, Walker AW. Reagent and laboratory contamination can critically impact sequence-based microbiome analyses. BMC Biol. 2014 Nov 12;12:87

[65] Moreno I, Codoñer FM, Vilella F, Valbuena D, Martinez-Blanch JF, Jimenez-Almazán J, Alonso R, Alamá P, Remohí J, Pellicer A, Ramon D, Simon C. Evidence that the endometrial microbiota has an effect on implantation success or failure. Am J Obstet Gynecol. 2016 Oct 4. pii: S0002-9378(16)30782-7.

[66] Fang RL, Chen LX, Shu WS, Yao SZ, Wang SW, Chen YQ. Barcoded sequencing reveals diverse intrauterine microbiomes in patients suffering with endometrial polyps. Am J Transl Res. 2016 Mar 15;8(3):1581-92.

[67] Marconi C, de Andrade Ramos BR, Peracoli JC, Donders GG, da Silva MG. Amniotic fluid interleukin-1 beta and interleukin-6, but not interleukin-8 correlate with microbial invasion of the amniotic cavity in preterm labor. Am J Reprod Immunol (2011) 65(6):549–56.

[68] Chiang T, Duncan FE, Schindler K, Schultz RM, Lampson MA. Evidence that weakened centromere cohesion is a leading cause of age-related aneuploidy in oocytes. Curr Biol 2010; 20:1522-1528.

[69] Duncan FE, Chiang T, Schultz RM, Lampson MA. Evidence that a defective spindle assembly checkpoint is not the primary cause of maternal age-associated aneuploidy in mouse eggs. Biol Reprod 2009; 81:768-776.

[70] Merriman JA, Jennings PC, McLaughlin EA, Jones KT. Effect of aging on superovulation efficiency, aneuploidy rates, and sister chromatid cohesion in mice aged up to 15 months. Biol Reprod 2012; 86:49.

[71] Handyside AH, Montag M, Magli MC, Repping S, Harper J, Schmutzler A, Vesela K, Gianaroli L, Geraedts J. Multiple meiotic errors caused by predivision of chromatids in women of advanced maternal age undergoing in vitro fertilisation. Eur J Hum Genet 2012; 20:742-747.

[72] Fragouli E, Alfarawati S, Goodall NN, Sanchez-Garcia JF, Colls P, Wells D. The cytogenetics of polar bodies: insights into female meiosis and the diagnosis of aneuploidy. Mol Hum Reprod 2011; 17:286-295.

[73] Duncan FE, Hornick JE, Lampson MA, Schultz RM, Shea LD, Woodruff TK. Chromosome cohesion decreases in human eggs with advanced maternal age. Aging Cell 2012; 11:1121-1124.

[74] Downs SM. Regulation of the G2/M transition in rodent oocytes. Mol Reprod Dev. 2010;77:566–85.

[75] Alexandra Sanfins, Carlos E. Plancha, David F. Albertini. Pre-implantation developmental potential from in vivo and in vitro matured mouse oocytes: a cytoskeletal perspective on oocyte quality. J Assist Reprod Genet. 2015;32: 127–136.

[76] Cheng-Jie Zhou, Sha-Na Wu, Jiang-Peng Shen, Dong-Hui Wang, Xiang-Wei Kong, Angeleem Lu, Yan-Jiao Li, Hong-Xia Zhou, Yue-Fang Zhao, Cheng-Guang Liang. The beneficial effects of cumulus cells and oocyte-cumulus cell gap junctions depends on oocyte maturation and fertilization methods in mice. PeerJ. 2016;4:e1761.

[77] Li Y, Feng HL, Cao YJ, Zheng GJ, Yang Y, Mullen S, Critser JK, Chen ZJ. Confocal microscopic analysis of the spindle and chromosome configurations of human oocytes matured in vitro. Fertil Steril 2006; 85:827-832.

[78] Wells D, Kaur K, Grifo J, Glassner M, Taylor JC, Fragouli E, Munne S. Clinical utilisation of a rapid low-pass whole genome sequencing technique for the diagnosis of aneuploidy in human embryos prior to implantation. J Med Genet 2014; 51:553-562.

[79] Dalton CM, Carroll J. Biased inheritance of mitochondria during asymmetric cell division in the mouse oocyte. J Cell Sci. 2013;126:2955-64.

[80] Piko L, Taylor KD. Amounts of mitochondrial DNA and abundance of some mitochondrial gene transcripts in early mouse embryos. Dev Biol. 1987;123:364–74.

[81] Thundathil J, Filion F, Smith LC. Molecular control of mitochondrial function in preimplantation mouse embryos. Mol Reprod Dev. 2005;71:405-13.

[82] St John JC, Facucho-Oliveira J, Jiang Y, Kelly R, Salah R. Mitochondrial DNA transmission, replication and inheritance: a journey from the gamete through the embryo and into offspring and embryonic stem cells. Hum Reprod Update. 2010;16:488-509.

[83] Wang Q, Ratchford AM, Chi MM, Schoeller E, Frolova A, Schedl T, Moley KH. Maternal diabetes causes mitochondrial dysfunction and meiotic defects in murine oocytes. Mol Endocrinol. 2009;23:1603-12.

[84] Leese HJ, Baumann CG, Brison DR, McEvoy TG, Sturmey RG. Metabolism of the viable mammalian embryo: quietness revisited. Mol Hum Reprod. 2008;14:667-72.

[85] Leese HJ. Metabolism of the preimplantation embryo: 40 years on. Reproduction. 2012;143:417-27.

[86] Rambags BP, van Boxtel DC, Tharasanit T, Lenstra JA, Colenbrander B, Stout TA. Advancing maternal age predisposes to mitochondrial damage and loss during maturation of equine oocytes in vitro. Theriogenology. 2014;81:959-65.

[87] Iwata H, Goto H, Tanaka H, Sakaguchi Y, Kimura K, Kuwayama T, Monji Y. Effect of maternal age on mitochondrial DNA copy number, ATP content and IVF outcome of bovine oocytes. Reprod Fertil Dev. 2011;23:424-32.

[88] Wang LY, Wang DH, Zou XY, Xu CM. Mitochondrial functions on oocytes and preimplantation embryos. J Zhejiang Univ Sci B. 2009;10:483-92.

[89] Diez-Juan A, Rubio C, Marin C, Martinez S, Al-Asmar N, Riboldi M, Díaz-Gimeno P, Valbuena D, Simón C. Mitochondrial DNA content as a viability score in human euploid embryos: less is better. Fertil Steril. 2015;104:534-41.

[90] Tolkovsky AM, Xue L, Fletcher GC, Borutaite V. Mitochondrial disappearance from cells: a clue to the role of autophagy in programmed cell death and disease? Biochimie. 2002;84:233-40.

[91] Lemasters JJ. Selective mitochondrial autophagy, or mitophagy, as a targeted defense against oxidative stress, mitochondrial dysfunction, and aging. Rejuvenation Res. 2005;8:3-5.

[92] Alexandra Sanfins, Carlos E. Plancha, David F. Albertini. Pre-implantation developmental potential from in vivo and in vitro matured mouse oocytes: a cytoskeletal perspective on oocyte quality. J Assist Reprod Genet. 2015;32: 127–136.

[93] Cheng-Jie Zhou, Sha-Na Wu, Jiang-Peng Shen, Dong-Hui Wang, Xiang-Wei Kong, Angeleem Lu, Yan-Jiao Li, Hong-Xia Zhou, Yue-Fang Zhao, Cheng-Guang Liang. The beneficial effects of cumulus cells and oocyte-cumulus cell gap junctions depends on oocyte maturation and fertilization methods in mice. PeerJ. 2016;4:e1761.

[94] Reynier P, May-Panloup P, Chrétien MF, Morgan CJ, Jean M, Savagner F, Barrière P, Malthièry Y. Mitochondrial DNA content affects the fertilizability of human oocytes. Mol Hum Reprod. 2001;7:425-9.

[95] Fragouli E, Spath K, Alfarawati S, Kaper F, Craig A, Michel CE et al. Altered levels of mitochondrial DNA are associated with female age, aneuploidy, and provide an independent measure of embryonic implantation potential. PLoS genetics. 2015;11(6):e1005241. doi:10.1371/journal.pgen.1005241.

[96] Scott RT, Jr., Upham KM, Forman EJ, Zhao T, Treff NR. Cleavage-stage biopsy significantly impairs human embryonic implantation potential while blastocyst biopsy does not: a randomized and paired clinical trial. Fertil Steril. 2013;100(3):624-30.

[97] Forman EJ, Li X, Ferry KM, Scott K, Treff NR, Scott RT, Jr. Oocyte vitrification does not increase the risk of embryonic aneuploidy or diminish the implantation potential of blastocysts created after intracytoplasmic sperm injection: a novel, paired randomized controlled trial using DNA fingerprinting. Fertil Steril. 2012;98(3):644-9.

[98] Scott RT, Jr., Ferry K, Su J, Tao X, Scott K, Treff NR. Comprehensive chromosome screening is highly predictive of the reproductive potential of human embryos: a prospective, blinded, nonselection study. Fertil Steril 2012;97(4):870-5.

[99]Franasiak JM, Werner MD, Juneau CR, Tao X, Landis J, Zhan Y, Treff NR, Scott RT. Endometrial microbiome at the time of embryo transfer: next-generation sequencing of the 16S ribosomal subunit. J Assist Reprod Genet. 2016 Jan;33(1):129-36. doi: 10.1007

[100] Franasiak JM, Werner MD, Juneau CR, Tao X, Landis J, Zhan Y, Treff NR, Scott RT. Endometrial microbiome at the time of embryo transfer: next-generation sequencing of the 16S ribosomal subunit. J Assist Reprod Genet. 2016 Jan;33(1):129-36. doi: 10.1007